Supporting Information

Structure, assembly mechanism and magnetic properties of heterometallic dodecanuclear nanoclusters $Dy^{III}_4M^{II}_8$ (M = Ni, Co)

Shui Yu,[†] Qin-Hua Zhang,‡ Zilu Chen,[*,†] Hua-Hong Zou,[†] Huancheng Hu,[†] Dongcheng Liu,[†] Fu-Pei Liang[*,†,§]

[†]State Key Laboratory for Chemistry and Molecular Engineering of Medicinal Resources, Collaborative Innovation Center for Guangxi Ethnic Medicine, School of Chemistry and Pharmaceutical Sciences, Guangxi Normal University, Guilin 541004, P. R. China. E-mail: zlchen@mailbox.gxnu.edu.cn; fliangoffice@yahoo.com

[‡]State Key Laboratory of Heavy Oil Processing, Institute of New Energy, College of Chemical Engineering, China University of Petroleum (East China), Qingdao 266580, P. R. China.

[§]Guangxi Key Laboratory of Electrochemical and Magnetochemical Functional Materials, College of Chemistry and Bioengineering, Guilin University of Technology, Guilin, 541004, P. R. China. E-mail: fliangoffice@yahoo.com

Experimental

Materials and Measurements.

All chemical reagents were used as commercially received without further purification. The Fourier transform infrared (FT-IR) data of the two complexes were collected on Perkin-Elmer Spectrum One FT-IR spectrometer using the corresponding KBr Pellets in the wavenumber range of 4000-400 cm^{-1} (Fig S1-S2). The powder X-ray diffraction (PXRD) measurements were carried out on a Rigaku D/max 2500v/pc diffractometer equipped with Cu-Kα radiation (λ = 1.5418 Å) at 40 kV and 40 mA, with a step size of 0.02° in 2θ and a scan speed of 5° min^{-1}. Elemental analyses for C, H, and N for the two complexes were performed on an Elementar Micro cube C, H, N elemental analyzer. The TG analyses (30-1000 °C) for **1** and **2** were conducted on a PerkinElmer Diamond TG/DTA thermal analyzer in a flowing nitrogen atmosphere with a heating rate of 5 °C min^{-1}. All magnetic data were measured on a Quantum Design MPMS SQUID-XL-7 SQUID magnetometer furnished with a 7 T and 5 T magnets. The magnetic data of the two complexes were corrected with a consideration of diamagnetic contribution from the sample and the sample holder.

Single-crystal X-ray crystallography.

Diffraction data for these complexes were collected on a Bruker SMART CCD diffractometer (Mo Kα radiation and λ= 0.71073 Å) in Φ and ω scan modes. The structures were solved by direct methods, followed by difference Fourier syntheses, and then refined by full-matrix least-squares techniques on F2 using SHELXL. All other non-hydrogen atoms were refined with anisotropic thermal parameters.

Hydrogen atoms were placed at calculated positions and isotropically refined using a riding model. Table S1 summarizes X-ray crystallographic data and refinement details for the complexes. Full details can be found in the CIF files provided in the Supporting Information. The CCDC reference numbers are 2092954 and 2092955.

ESI-MS measurement.

ESI-MS measurements were conducted at a capillary temperature of 275 °C. Aliquots of the solution were injected into the device at 0.3 mL/h. The mass spectrometer used for the measurements was a Thermo Exactive, and the data were collected in positive and negative ion modes. The spectrometer was previously calibrated with the standard tune mix to give a precision of ca. 2 ppm within the region of 200−2,000 m/z. The capillary voltage was 50 V, the tube lens voltage was 150 V, and the skimmer voltage was 25 V. The in-source energy was set within the range of 0-100 eV with a gas flow rate at 10% of the maximum.

Synthesis and characterization

The reactions of 1-[[(2-Hydroxyethyl)imino]methyl]-2-naphthalenol with $Co(OAc)_2 \cdot 4H_2O$ and $Dy(NO)_3 \cdot 6H_2O$, or with $Ni(OAc)_2 \cdot 4H_2O$ in acetonitrile in sealed Pyrex tube at 80 ºC afforded $[Dy_4Co_8(\mu_3\text{-}OH)_8(L)_8(OAc)_4(H_2O)_4] \cdot 3EtOH \cdot 3CH_3CN \cdot H_2O$ (**1**) $[Dy_4Ni_8(\mu_3\text{-}OH)_8(L)_8(OAc)_4(H_2O)_4] \cdot 3.5EtOH \cdot 0.5CH_3CN \cdot 5H_2O$ (**2**) in crystalline forms, respectively. The increasing the reaction temperature to 100 ºC resulted in much poorer crystal quality and much lower yield. When the reaction temperature was lowered to 70 °C, no crystalline products of the two titled complexes were found. The change of the mixed solvents into the sole solvent of ethanol or acetonitrile, as well as the change of the reaction method into routine solution method, also failed to obtain the two titled complexes. The TG analyses of **1** and **2** are shown in Fig. S5 and S6, respectively. Upon increasing the temperature from ambient temperature, complex **1** underwent a slow weight loss of 15.40% before 231 ºC with a subsequent much faster weight loss, which corresponds to the loss of three free ethanol, three acetonitrile, one water molecules and four coordinated OAc^- and four water molecules (calcd 15.79%) per formular unit of **1**. The followed weight losses were due to the collapse of the Schiff base ligands in **1**, which didn't come to an end even when the temperature was raised at 1000 ºC. Upon increasing the temperature from ambient temperature, complex **2** underwent a slow weight loss of 13.04% before 257 ºC with a subsequent much faster weight loss, which corresponds to the loss of thtree point five free ethanol, zero point five acetonitrile, five water molecules and two coordinated OAc^- and four water molecules (calcd 13.03%) per formular unit of **2**. The followed loss of the Schiff base was not complete even when the sample was heated to 1000 ºC. The purities of the collected bulky crystalline samples of complexes **1** and **2** were confirmed by the nice agreement of the experimental PXRD curves with the simulated ones derived from the corresponding single crystal X-ray diffraction data as shown in Fig. S3 and S4, respectively.

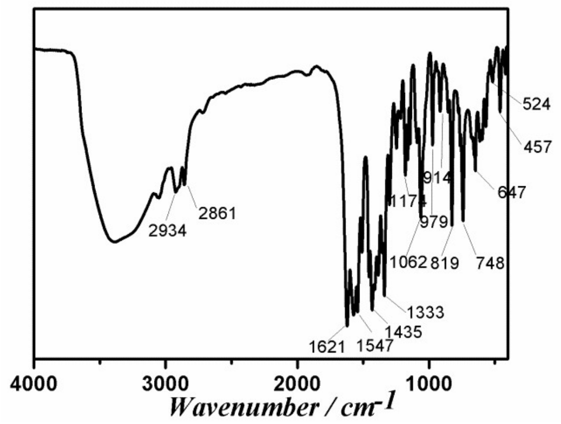

Fig. S1 FT-IR spectrum of **1**.

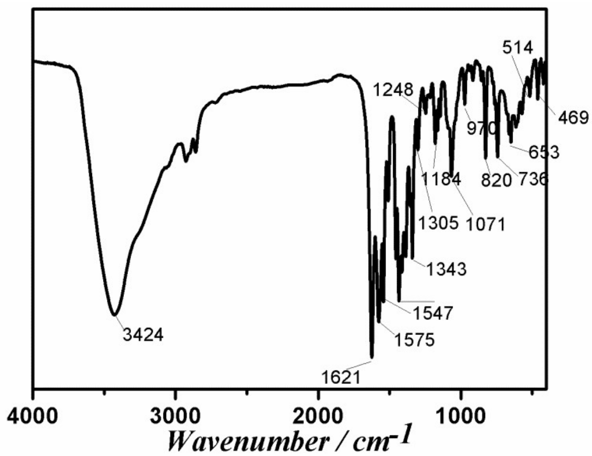

Fig. S2 FT-IR spectrum of **2**.

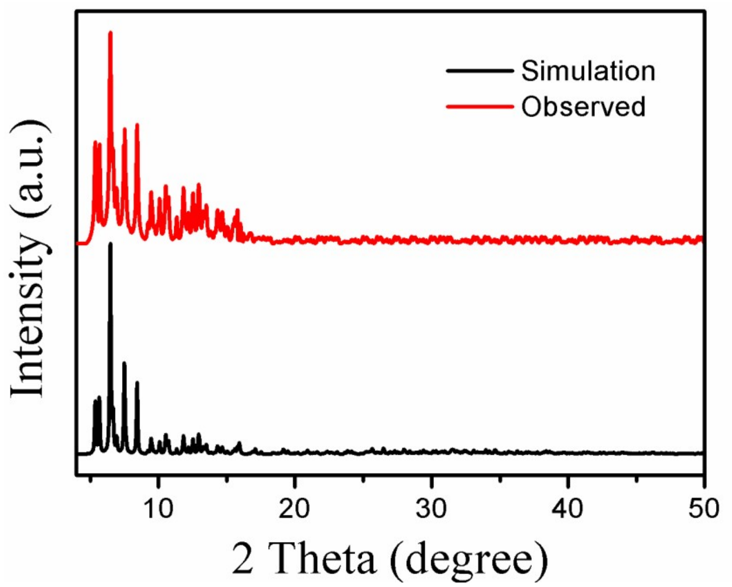

Fig. S3. PXRD patterns of **1**.

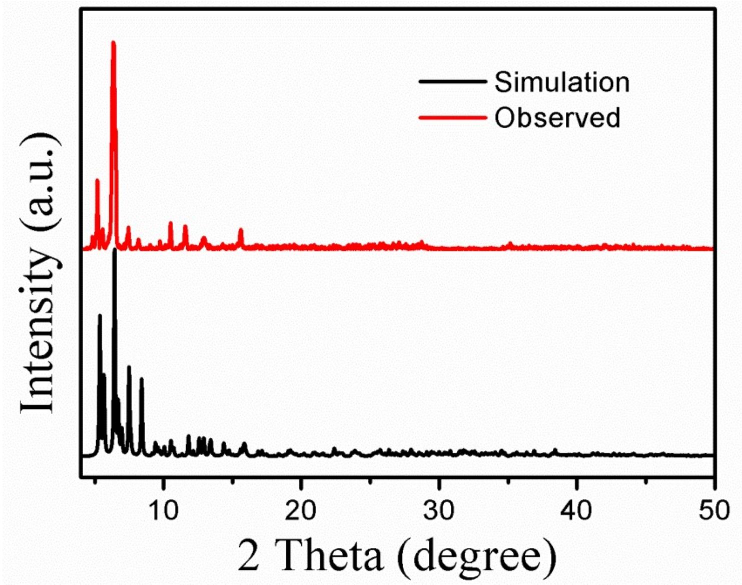

Fig. S4. PXRD patterns of **2**.

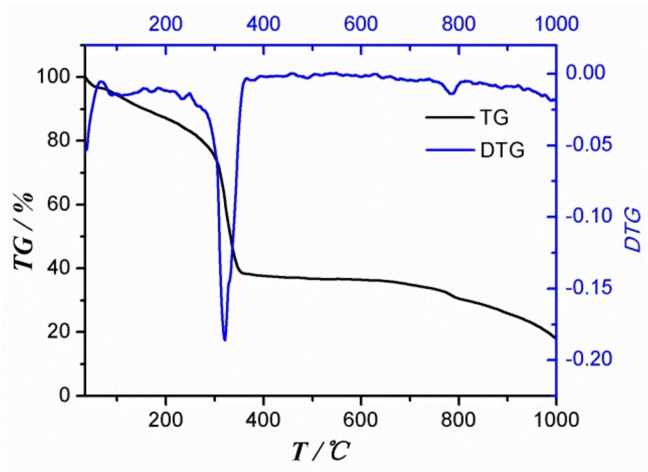

Fig. S5. The TG curve for **1**.

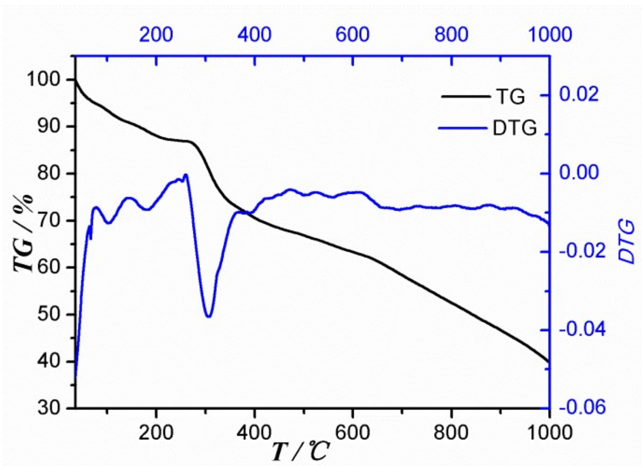

Fig. S6. The TG curve for **2**.

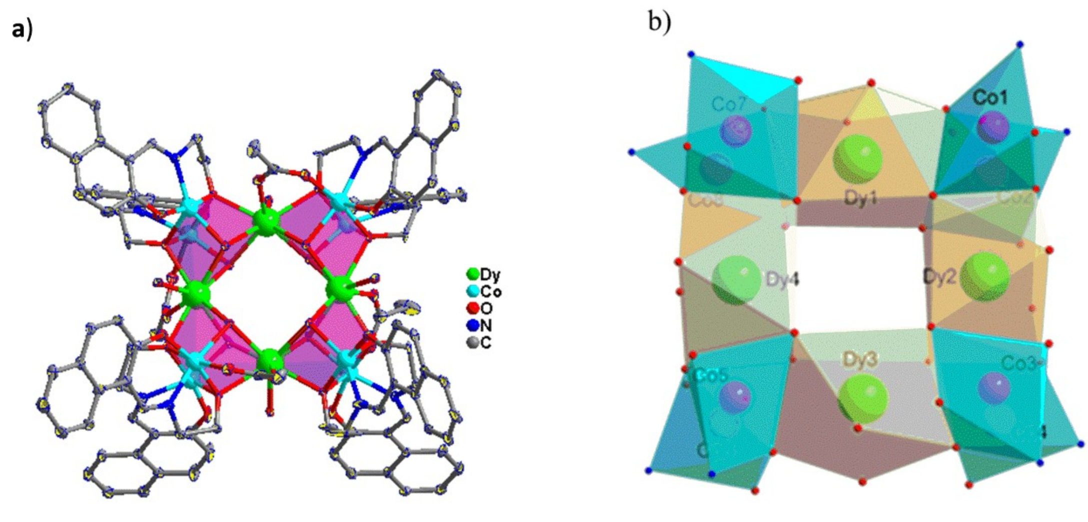

Fig. S7. The structure of **1** with 30 % probability ellipsoid (a) and molecular skeleton filling diagram (b). Hydrogen atoms are omitted for clarity.

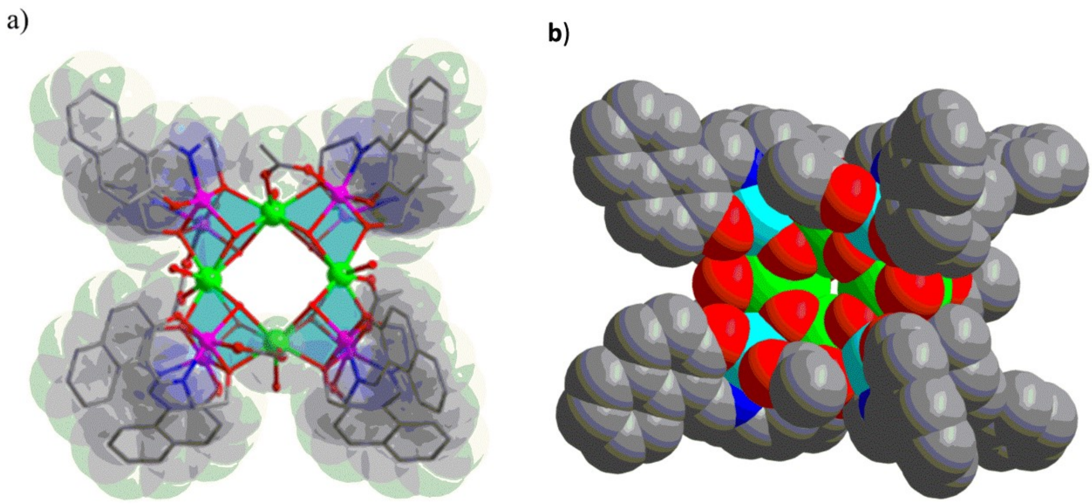

Fig. S8. Molecular fill map of **1**.

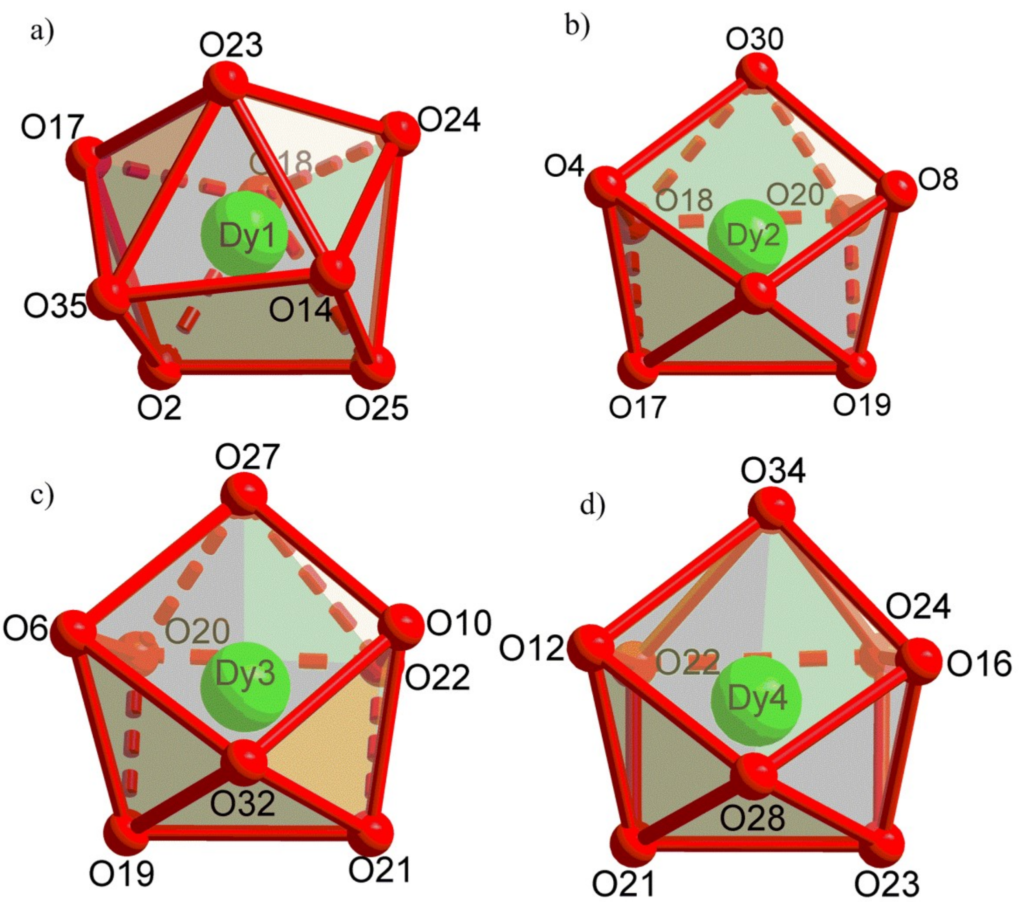

Fig. S9. Coordination polyhedron around the Dy(III) ion of **1** with labels for selected atoms.

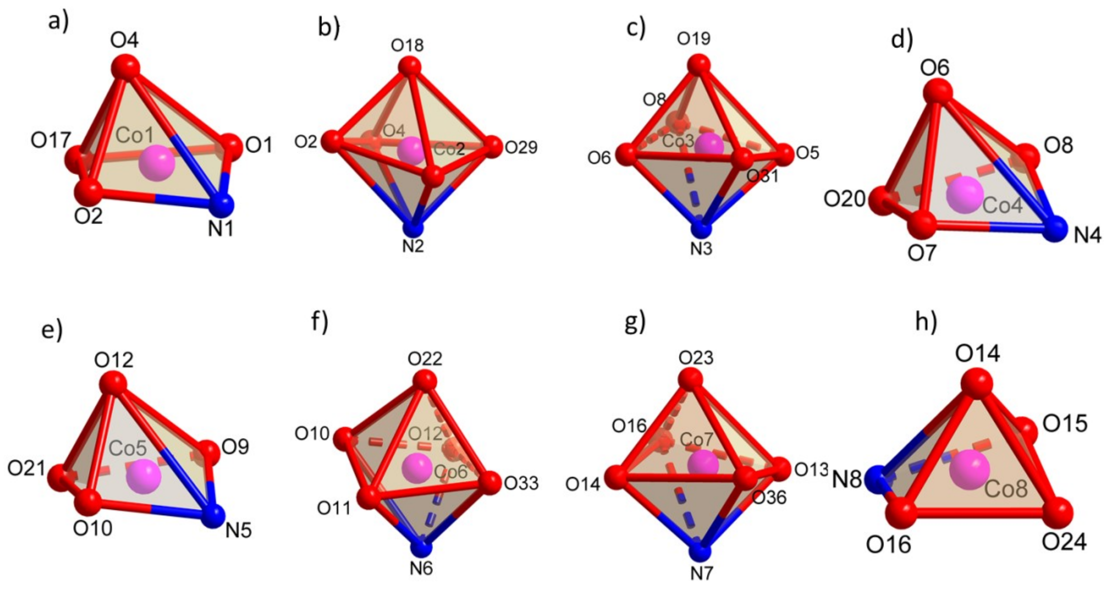

Fig. S10. Coordination polyhedron around the Co(II) ion of **1** with labels for selected atoms.

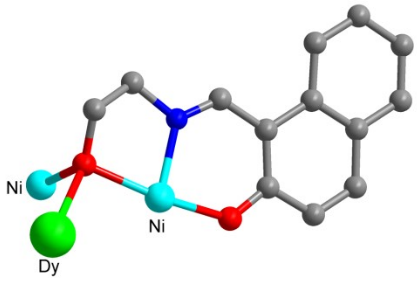

Fig. S11. Same bridging modes of L^{2-} in **1**.

Table S1. SHAPE analysis of Dy1 in **1**

Configuration	ABOXIY
Octagon (D_{8h})	27.660
Heptagonal pyramid (C_{7v})	21.380
Hexagonal bipyramid (D_{6h})	16.593
Cube (O_h)	9.927
Square antiprism (D_{4d})	**0.377**
Triangular dodecahedron (D_{2d})	2.112
Johnson gyrobifastigium J26 (D_{2d})	16.858
Johnson elongated triangular bipyramid J14 (D_{3H})	26.986
Biaugmented trigonal prism J50 (C_{2v})	2.763
Biaugmented trigonal prism (C_{2v})	2.062
Snub diphenoid J84 (D_{2d})	4.898
Triakis tetrahedron (T_d)	10.479
Elongated trigonal bipyramid (D_{3h})	22.416

Table S2. SHAPE analysis of Dy2 in **1**

Configuration	ABOXIY
Octagon (D_{8h})	27.401
Heptagonal pyramid (C_{7v})	21.684
Hexagonal bipyramid (D_{6h})	16.799
Cube (O_h)	9.856
Square antiprism (D_{4d})	**0.344**
Triangular dodecahedron (D_{2d})	2.335
Johnson gyrobifastigium J26 (D_{2d})	16.125
Johnson elongated triangular bipyramid J14 (D_{3H})	26.493
Biaugmented trigonal prism J50 (C_{2v})	2.753
Biaugmented trigonal prism (C_{2v})	2.143
Snub diphenoid J84 (D_{2d})	5.154
Triakis tetrahedron (T_d)	10.432
Elongated trigonal bipyramid (D_{3h})	21.802

Table S3. SHAPE analysis of Dy3 in **1**

Configuration	ABOXIY
Octagon (D_{8h})	27.687
Heptagonal pyramid (C_{7v})	21.408
Hexagonal bipyramid (D_{6h})	16.473
Cube (O_h)	9.938
Square antiprism (D_{4d})	**0.462**
Triangular dodecahedron (D_{2d})	2.043
Johnson gyrobifastigium J26 (D_{2d})	16.678
Johnson elongated triangular bipyramid J14 (D_{3H})	26.121
Biaugmented trigonal prism J50 (C_{2v})	2.730
Biaugmented trigonal prism (C_{2v})	2.082
Snub diphenoid J84 (D_{2d})	4.643
Triakis tetrahedron (T_d)	10.559
Elongated trigonal bipyramid (D_{3h})	21.498

Table S4. SHAPE analysis of Dy4 in **1**

Configuration	ABOXIY
Octagon (D_{8h})	27.647
Heptagonal pyramid (C_{7v})	21.432
Hexagonal bipyramid (D_{6h})	16.166
Cube (O_h)	9.609
Square antiprism (D_{4d})	**0.442**
Triangular dodecahedron (D_{2d})	2.184
Johnson gyrobifastigium J26 (D_{2d})	16.037
Johnson elongated triangular bipyramid J14 (D_{3H})	26.272
Biaugmented trigonal prism J50 (C_{2v})	2.926
Biaugmented trigonal prism (C_{2v})	2.295
Snub diphenoid J84 (D_{2d})	5.152
Triakis tetrahedron (T_d)	10.127
Elongated trigonal bipyramid (D_{3h})	21.495

Table S5. Selected bond lengths / Å and bond angles / ° for **1.**

Dy1-O17	2.367(5)	Dy2-O20	2.368(5)	Dy3-O12	2.345(5)
Dy1-O29	2.375(5)	Dy2-O34	2.370(4)	Dy3-O33	2.367(5)
Dy1-O2	2.376(4)	Dy2-O4	2.380(5)	Dy3-O6	2.377(5)

Dy1-O16	2.385(5)	Dy2-O8	2.383(5)	Dy3-O21	2.381(5)
Dy1-O31	2.386(5)	Dy2-O32	2.397(5)	Dy3-O35	2.396(5)
Dy1-O30	2.418(4)	Dy2-O31	2.411(5)	Dy3-O36	2.419-(5)
Dy1-O32	2.432(5)	Dy2-O27	2.418(5)	Dy3-O34	2.423-(5)
Dy1-O28	2.473(5)	Dy2-O33	2.419(5)	Dy3-O26	2.456(5)
Dy4-O23	2.366(5)	Co1-O1	1.967(6)	Co3-O7	1.958(6)
Dy4-O36	2.366(5)	Co1-N1	1.992(6)	Co3-N4	1.991(6)
Dy4-O14	2.371(5)	Co1-O32	2.064(5)	Co3-O8	2.074(5)
Dy4-O30	2.384(5)	Co1-O4	2.072(5)	Co3-O33	2.077(5)
Dy4-O10	2.392(5)	Co1-O2	2.089(5)	Co3-O6	2.115(5)
Dy4-O29	2.416(4)	Co2-O3	1.988(5)	Co4-O5	2.014(5)
Dy4-O35	2.432(5)	Co2-N2	2.037(6)	Co4-N3	2.023(6)
Dy4-O25	2.449(5)	Co2-O4	2.102(5)	Co4-O6	2.096(5)
Co5-N5	2.018(6)	Co2-O31	2.107(4)	Co4-O22	2.129(6)
Co5-O9	2.019(5)	Co2-O19	2.162(6)	Co4-O34	2.136(5)
Co5-O35	2.092(5)	Co2-O2	2.175(5)	Co4-O8	2.145(5)
Co5-O12	2.141(5)	Co7-O13	1.960(5)	Co8-O16	2.127(5)
Co5-O10	2.143(5)	Co7-N7	1.990(6)	Co8-O18	2.133(6)
Co5-O24	2.170(6)	Co7-O29	2.072(5)	Co8-O14	2.153(5)
Co6-O11	1.972(5)	Co7-O14	2.078(5)	O12-Dy3-O33	141.13(17)
Co6-N6	1.982(7)	Co7-O16	2.089(5)	O12-Dy3-O6	119.71(17)
Co6-O36	2.058-(5)	Co8-O15	1.999(5)	O33-Dy3-O6	72.86(18)
Co6-O10	2.065-(5)	Co8-N8	2.044(6)	O12-Dy3-O21	75.04(19)
Co6-O12	2.105(5)	Co8-O30	2.121(5)	O33-Dy3-O21	142.47(18)
O17-Dy1-O29	141.78(17)	O20-Dy2-O34	132.7(2)	O6-Dy3-O21	79.21(19)
O17-Dy1-O2	141.-(3)	O20-Dy2-O4	80.3(2)	O12-Dy3-O35	71.42(17)
O29-Dy1-O2-	142.03(16)	O34-Dy2-O4	145.84(17)	O33-Dy3-O35	80.70(16)
O17-Dy1-O16	79.03(18)	O20-Dy2-O8	72.8(2)	O6-Dy3-O35	147.26(17)
O29-Dy1-O16	72.10(16)	O34-Dy2-O8	71.96(17)	O21-Dy3-O35	132.58(18)
O2-Dy1-O16	119.02(16)	O4-Dy2-O8	121.08(17)	O12-Dy3-O36	74.38(17)
O17-Dy1-O31	133.84(18)	O20-Dy2-O32	142.91(19)	O33-Dy3-O36	119.13(16)
O29-Dy1-O31	80.48(16)	O34-Dy2-O32	81.05(15)	O6-Dy3-O36	143.33(17)
O2-Dy1-O31	72.81(16)	O4-Dy2-O32	70.93(16)	O21-Dy3-O36	72.06(17)
O16-Dy1-O31	146.16(16)	O8-Dy2-O32	142.72(17)	O35-Dy3-O36	67.32(16)
O17-Dy1-O30	80.64(17)	O20-Dy2-O31	82.26(18)	O12-Dy3-O34	148.70(16)
O29-Dy1-O30	67.72(16)	O34-Dy2-O31	114.01(16)	O33-Dy3-O34	67.87(16)
O2-Dy1-O30	148.41(16)	O4-Dy2-O31	73.13(16)	O6-Dy3-O34	73.55(16)
O16-Dy1-O30	73.73(16)	O8-Dy2-O31	147.48(17)	O21-Dy3-O34	80.63(17)
O31-Dy1-O30	113.86(15)	O32-Dy2-O31	67.50(16)	O35-Dy3-O34	113.97(16)
O17-Dy1-O32	73.25(18)	O20-Dy2-O27	112.60(19)	O36-Dy3-O34	79.62(16)
O29-Dy1-O32	119.08(16)	O34-Dy2-O27	84.31(17)	O12-Dy3-O26	70.22(17)
O2-Dy1-O32	74.64(16)	O4-Dy2-O27	72.57(16)	O33-Dy3-O26	80.68(18)
O16-Dy1-O32	144.27(16)	O8-Dy2-O27	71.36(17)	O6-Dy3-O26	72.98(18)

O31-Dy1-O32.	67.33(16)	O32-Dy2-O27	80.98(17)	O21-Dy3-O26	114.60(19)
O30-Dy1-O32	79.84(16)	O31-Dy2-O27	139.27(16)	O35-Dy3-O26	84.16(17)
O17-Dy1-O28	116.32(18)	O20-Dy2-O33	72.48(19)	O36-Dy3-O26	140.08(17)
O29-Dy1-O28	78.81(16)	O34-Dy2-O33	67.90(16)	O34-Dy3-O26-	139.35(16)
O2-Dy1-O28	71.45(16)	O4-Dy2-O33	143.79(17)	O12-Dy3-O33	141.13(17)
O16-Dy1-O28.	73.24(16)	O8-Dy2-O33	73.11(18)	O12-Dy3-O6	119.71(17)
O31-Dy1-O28	82.45(16)	O32-Dy2-O33	119.85(16)	O33-Dy3-O6	72.86(18)
O30-Dy1-O28	138.58(16)	O31-Dy2-O33	79.82(16)	O12-Dy3-O21	75.04(19)
O32-Dy1-O28	139.84(16)	O27-Dy2-O33	140.14(17)	O33-Dy3-O21	142.47(18)
O17-Dy1-O29	141.78(17)-.	O20-Dy2-O33	88.14(16)	O6-Dy3-O21	79.21(19)
O17-Dy1-O2	74.45(18)	O34-Dy2-O33	74.74(11)	O12-Dy3-O35	71.42(17)
O29-Dy1-O2	142.03(16)	O20-Dy2-O34	132.7(2)	O33-Dy3-O35	80.70(16)
O17-Dy1-O16.	79.03(18)	O20-Dy2-O4	80.3(2)	O6-Dy3-O35	147.26(17)
O29-Dy1-O16	72.10(16)	O34-Dy2-O4	145.84(17	O21-Dy3-O35	132.58(18)
O2-Dy1-O16	119.02(16)	O20-Dy2-O8	72.8(2)	O12-Dy3-O36-	74.38(17)
O17-Dy1-O31	133.84(18)	O34-Dy2-O8	71.96(17)	O33-Dy3-O36	119.13(16)
O29-Dy1-O31	80.48(16)	O4-Dy2-O8	121.08(17)	O6-Dy3-O36	143.33(17)
O2-Dy1-O31	72.81(16)	O20-Dy2-O32	142.91(19)	O21-Dy3-O36	72.06(17)
O16-Dy1-O31	146.16(16)	O34-Dy2-O32	81.05(15)	O35-Dy3-O36	67.32(16)
O17-Dy1-O30	80.64(17)	O4-Dy2-O32	70.93(16)	O12-Dy3-O34	148.70(16)
O29-Dy1-O30	67.72(16)	O8-Dy2-O32	142.72(17)	O33-Dy3-O34	67.87(16)
O2-Dy1-O30	148.41(16)	O20-Dy2-O31	82.26(18)	O6-Dy3-O34	73.55(16)
O16-Dy1-O30.	73.73(16)	O34-Dy2-O31	114.01(16)	O21-Dy3-O34	80.63(17)
O31-Dy1-O30.	113.86(15)	O4-Dy2-O31	73.13(16)	O35-Dy3-O34	113.97(16)
O23-Dy4-O36	141.85(18)	O1-Co1-N1	89.9(2)	O3-Co2-O2	93.1(2)
O23-Dy4-O14	72.75(18)	O1-Co1-O32	100.7(2)	N2-Co2-O2	100.1(2)
O36-Dy4-O14	143.33(16)	N1-Co1-O32	151.2(2)	O4-Co2-O2	80.0(2)
O23-Dy4-O30	133.69(17)	O1-Co1-O4	96.1(2)	O31-Co2-O2	82.57(18)
O36-Dy4-O30	81.95(16)-.	N1-Co1-O4	121.6(2)	O19-Co2-O2	171.1(2)
O14-Dy4-O30	71.46(16)-.	O32-Co1-O4	84.16(19)	O7-Co3-N4	89.5(3)
O23-Dy4-O10	77.87(18)-.	O1-Co1-O2	169.9(2)	O7-Co3-O8	172.2(3)
O36-Dy4-O10	71.63(17)-.	N1-Co1-O2	82.4(2)	N4-Co3-O8	83.1(2)
O14-Dy4-O10	120.30(16)	O32-Co1-O2	89.15(18)	O7-Co3-O33	100.7(3)
O30-Dy4-O10	146.83(16)	O4-Co1-O2	82.73(19)	N4-Co3-O33	154.6(2)
O23-Dy4-O29	74.74(17)-.	O3-Co2-N2	87.8(2)	O8-Co3-O33	87.1(2)
O36-Dy4-O29	119.31(16)	O3-Co2-O4	165.3(2)	O7-Co3-O6	99.8(3)
O14-Dy4-O29	73.46(16)-.	N2-Co2-O4	80.7(2)	N4-Co3-O6	116.9(2)
O30-Dy4-O29	67.62(15)-.	O3-Co2-O31	106.7(2)	O8-Co3-O6	81.6(2)
O10-Dy4-O29	143.47(16)	N2-Co2-O31	165.1(2)	O33-Co3-O6	84.43(19)
O23-Dy4-O35	82.21(17)-.	O4-Co2-O31	85.39(18)	O5-Co4-N3	88.8(2)
O36-Dy4-O35	67.59(16)-.	O3-Co2-O19	87.4(2)	O5-Co4-O6	166.4(2)
O14-Dy4-O35	146.96(16)	N2-Co2-O19	88.8(2)	N3-Co4-O6	82.1(2)
O30-Dy4-O35	115.03(16)	O4-Co2-O19	101.5(2)	O5-Co4-O22	90.4(2)

O10-Dy4-O35	73.24(16)-.	O31-Co2-O1	88.8(2)	N3-Co4-O22	90.7(3)
O29-Dy4-O35	79.47(16)-.	O6-Co4-O22	99.7(2)	O12-Co5-O2	171.7(2)
O23-Dy4-O25	112.75(18)	O5-Co4-O34	103.9(2)	O10-Co5-O2	100.2(2)
O36-Dy4-O25	80.06(17)-.	N3-Co4-O34	167.3(2)	O11-Co6-N6	90.4(3)
O14-Dy4-O25	72.06(16)-.	O6-Co4-O34	85.56(18)	O11-Co6-O3	99.2(2)
O30-Dy4-O25	82.70(16)-.	O22-Co4-O3	88.7(2)	N6-Co6-O36	151.9(3)
O10-Dy4-O25	73.47(16)-.	O5-Co4-O8	91.2(2)	O11-Co6-O1	103.2(2)
O29-Dy4-O25	140.05(16)	N3-Co4-O8	99.1(2)	N6-Co6-O10	118.6(3)
O35-Dy4-O25	139.24(16)	O6-Co4-O8	80.4(2)	O36-Co6-O1	84.99(19)
O15-Co8-O3	106.23(19)	O22-Co4-O8	170.1(2)	O11-Co6-O1	171.6(2)
N8-Co8-O30	164.9(2)	O34-Co4-O8	81.43(18)	N6-Co6-O12	81.3(2)
O15-Co8-O1	162.6(2)	N5-Co5-O9	87.8(2)	O36-Co6-O1	87.59(19)
N8-Co8-O16	81.0(2)	N5-Co5-O35	165.4(2)	O10-Co6-O1	82.2(2)
O30-Co8-O1	85.45(18)	O9-Co5-O35	106.1(2)	O13-Co7-N7	89.6(2)
O15-Co8-O1	92.8(2)	N5-Co5-O12	102.4(2)	O13-Co7-O2	98.0(2)
N8-Co8-O18	86.1(2)	O9-Co5-O12	91.9(2)	N7-Co7-O29	156.6(2)
O30-Co8-O1	89.9(2)	O35-Co5-O1	81.65(18)	O13-Co7-O1	171.3(2)
O16-Co8-O1	100.26(19)	N5-Co5-O10	81.5(2)	N7-Co7-O14	82.9(2)
O15-Co8-O1	88.8(2)	O9-Co5-O10	164.4(2)	O29-Co7-O1	87.21(19)
N8-Co8-O14	102.9(2)	O35-Co5-O1	85.60(18)	O13-Co7-O1	104.5(2)
O30-Co8-O1	81.04(18)	O12-Co5-O1	79.5(2)	N7-Co7-O16	114.9(2)
O16-Co8-O1	80.17(18)	N5-Co5-O24	85.7(2)	O29-Co7-O1	84.63(19)
O18-Co8-O1	170.9(2)	O9-Co5-O24	90.2(2)	O14-Co7-O1	82.79(19)
		O35-Co5-O2	90.1(2)	O15-Co8-N8	88.5(2)

Table S6. Selected bond lengths / Å and bond angles / ° for **2.**

Dy1-O31	2.314-(6)	Dy2-O34	2.347-(6)	Dy3-O33	2.304-(6)
Dy1-O2	2.331-(6)	Dy2-O32	2.356-(6)	Dy3-O6	2.334-(6)
Dy1-O29	2.335-(6)	Dy2-O8	2.357-(6)	Dy3-O12	2.355-(6)
Dy1-O16	2.356-(6)	Dy2-O4	2.363-(6)	Dy3-O21	2.363-(7)
Dy1-O17	2.375-(8)	Dy2-O27	2.386-(7)	Dy3-O35	2.376-(6)
Dy1-O32	2.388-(6)	Dy2-O20	2.388-(8)	Dy3-O36	2.393-(6)
Dy1-O30	2.390-(6)	Dy2-O33	2.391-(6)	Dy3-O34	2.415-(6)
Dy1-O28	2.431-(6)	Dy2-O31	2.392-(6)	Dy3-O26	2.433-(7)
Dy4-O36	2.312-(6)	Ni1-N1	1.964-(8)	Ni3-N4	1.964-(8)
Dy4-O30	2.328-(6)	Ni1-O1	1.989-(7)	Ni3-O7	1.964-(7)
Dy4-O23	2.362-(7)	Ni1-O2	2.054-(6)	Ni3-O8	2.030-(6)
Dy4-O10	2.364-(6)	Ni1-O32	2.063-(6)	Ni3-O33	2.051-(6)
Dy4-O14	2.380-(6)	Ni1-O4	2.106-(7)	Ni3-O6	2.110-(6)
Dy4-O29	2.383-(6)	Ni1-O18	2.193-(8)	Ni4-N3	1.996-(8)
Dy4-O35	2.402-(6)	Ni2-O3	1.987-(7)	Ni4-O5	2.020-(7)

Dy4-O25	2.435-(6)	Ni2-N2	1.990-(8)	Ni4-O34	2.080-(6)
Ni5-N5	1.972-(8)	Ni2-O4	2.064-(6)	Ni4-O6	2.085-(6)
Ni5-O9	2.010-(7)	Ni2-O31	2.079-(6)	Ni4-O22	2.086-(7)
Ni5-O35	2.066-(6)	Ni2-O19	2.136-(8)	Ni4-O8	2.096-(7)
Ni5-O12	2.092-(6)	Ni2-O2	2.159-(6)	Ni8-O30	2.065-(6)
Ni5-O10	2.106-(6)	Ni7-O13	1.960-(7)	Ni8-O14	2.069-(6)
Ni5-O24	2.130-(7)	Ni7-N7	1.965-(8)	Ni8-O16	2.072-(6)
Ni6-N6	1.959-(8)	Ni7-O16	2.043-(6)	O21-Dy3-O34	81.7(2)
Ni6-O11	1.980-(6)	Ni7-O29	2.045-(6)	O35-Dy3-O34	116.3(2)
Ni6-O36	2.024-(6)	Ni7-O14	2.059-(6)	O36-Dy3-O34	78.8(2)
Ni6-O12	2.052-(6)	Ni8-O15	1.962-(8)	O33-Dy3-O26	82.3(2)
Ni6-O10	2.069-(6)	Ni8-N8	1.969-(8)	O6-Dy3-O26	73.0(2)
O31-Dy1-O2	73.0(2)	O4-Dy2-O27	73.2(2)	O12-Dy3-O26	70.3(2)
O31-Dy1-O29	83.1(2)	O34-Dy2-O20	125.8(2)	O21-Dy3-O26	114.1(2)
O2-Dy1-O29	146.0(2)	O32-Dy2-O20	144.6(2)	O35-Dy3-O26	82.6(2)
O31-Dy1-O16	144.6(2)	O8-Dy2-O20	68.6(2)	O36-Dy3-O26	140.4(2)
O2-Dy1-O16	117.9(2)	O4-Dy2-O20	84.0(2)	O34-Dy3-O26	139.8(2)
O29-Dy1-O16	70.3(2)	O27-Dy2-O20	115.6(2)	O36-Dy4-O30	84.5(2)
O31-Dy1-O17	145.3(3)	O34-Dy2-O33	66.9(2)	O36-Dy4-O23	145.4(2)
O2-Dy1-O17	84.4(3)	O32-Dy2-O33	118.3(2)	O30-Dy4-O23	127.4(2)
O29-Dy1-O17	127.0(3)	O8-Dy2-O33	75.2(2)	O36-Dy4-O10	72.0(2)
O16-Dy1-O17	69.6(3)	O4-Dy2-O33	142.6(2)	O30-Dy4-O10	149.4(2)
O31-Dy1-O32	69.1(2)	O27-Dy2-O33	141.5(2)	O23-Dy4-O10	81.0(2)
O2-Dy1-O32	75.0(2)	O20-Dy2-O33	69.1(2)	O36-Dy4-O14	143.2(2)
O29-Dy1-O32	118.9(2)	O34-Dy2-O31	117.2(2)	O30-Dy4-O14	69.7(2)
O16-Dy1-O32	144.7(2)	O32-Dy2-O31	68.3(2)	O23-Dy4-O14	69.6(2)
O17-Dy1-O32	79.9(2)	O8-Dy2-O31	144.7(2)	O10-Dy4-O14	119.4(2)
O31-Dy1-O30	115.2(2)	O4-Dy2-O31	73.2(2)	O36-Dy4-O29	118.7(2)
O2-Dy1-O30	145.9(2)	O27-Dy2-O31	140.3(2)	O30-Dy4-O29	66.9(2)
O29-Dy1-O30	66.7(2)	O20-Dy2-O31	81.1(2)	O23-Dy4-O29	71.7(2)
O16-Dy1-O30	75.8(2)	O33-Dy2-O31	77.3(2)	O10-Dy4-O29	141.9(2)
O17-Dy1-O30	70.9(3)	O33-Dy3-O6	72.4(2)	O14-Dy4-O29	75.4(2)
O32-Dy1-O30	77.7(2)	O33-Dy3-O12	142.3(2)	O36-Dy4-O35	68.7(2)
O31-Dy1-O28	81.1(2)	O6-Dy3-O12	120.6(2)	O30-Dy4-O35	115.8(2)
O2-Dy1-O28	73.1(2)	O33-Dy3-O21	144.1(2)	O23-Dy4-O35	83.5(2)
O29-Dy1-O28	79.6(2)	O6-Dy3-O21	82.0(2)	O10-Dy4-O35	74.0(2)
O16-Dy1-O28	71.6(2)	O12-Dy3-O21	72.8(2)	O14-Dy4-O35	146.2(2)
O17-Dy1-O28	117.6(2)	O33-Dy3-O35	81.6(2)	O29-Dy4-O35	76.9(2)
O32-Dy1-O28	141.3(2)	O6-Dy3-O35	146.2(2)	O36-Dy4-O25	79.4(2)
O30-Dy1-O28	139.2(2)	O12-Dy3-O35	69.9(2)	O30-Dy4-O25	81.2(2)
O34-Dy2-O32	85.3(2)	O21-Dy3-O35	130.2(2)	O23-Dy4-O25	114.8(2)
O34-Dy2-O8	70.9(2)	O33-Dy3-O36	116.8(2)	O10-Dy4-O25	75.6(2)
O32-Dy2-O8	145.7(2)	O6-Dy3-O36	143.9(2)	O14-Dy4-O25	71.2(2)

O34-Dy2-O4	148.5(2)	O12-Dy3-O36	75.0(2)	O29-Dy4-O25	140.0(2)
O32-Dy2-O4	70.7(2)	O21-Dy3-O36	71.6(2)	O35-Dy4-O25	141.2(2)
O8-Dy2-O4-1	119.2(2)	O35-Dy3-O36	67.8(2)	O32-Dy2-O27	81.0(2)
O34-Dy2-O27	83.3(2)	O33-Dy3-O34	67.2(2)	O8-Dy2-O27	72.2(2)
N1-Ni1-O1	91.7(3)	N4-Ni3-O33	164.9(3)	O9-Ni5-O24	89.9(3)
N1-Ni1-O2	83.3(3)	O7-Ni3-O33	93.8(3)	O35-Ni5-O2	91.3(3)
O1-Ni1-O2	173.7(3)	O8-Ni3-O33	90.5(2)	O12-Ni5-O2	172.7(3)
N1-Ni1-O32	169.4(3)	N4-Ni3-O6	111.1(3)	O10-Ni5-O2	97.9(3)
O1-Ni1-O32	96.9(3)	O7-Ni3-O6	96.6(3)	N6-Ni6-O11	90.4(3)
O2-Ni1-O32	88.5(2)	O8-Ni3-O6	82.4(3)	N6-Ni6-O36	160.6(4)
N1-Ni1-O4	103.6(3)	O33-Ni3-O6	82.3(2)	O11-Ni6-O3	95.7(3)
O1-Ni1-O4	94.4(3)	N3-Ni4-O5	90.2(3)	N6-Ni6-O12	83.5(3)
O2-Ni1-O4	83.0(2)	N3-Ni4-O34	168.1(3)	O11-Ni6-O1	173.8(3)
O32-Ni1-O4	81.9(2)	O5-Ni4-O34	101.6(3)	O36-Ni6-O1	90.3(2)
N1-Ni1-O18	84.4(3)	N3-Ni4-O6	82.7(3)	N6-Ni6-O10	113.0(4)
O1-Ni1-O18	85.5(3)	O5-Ni4-O6	169.3(3)	O11-Ni6-O1	98.4(3)
O2-Ni1-O18	97.9(3)	O34-Ni4-O6	85.7(2)	O36-Ni6-O1	84.4(2)
O32-Ni1-O1	90.2(3)	N3-Ni4-O22	89.6(3)	O12-Ni6-O1	83.5(2)
O4-Ni1-O18	172.0(3)	O5-Ni4-O22	88.3(3)	O13-Ni7-N7	91.4(3)
O3-Ni2-N2	90.3(3)	O34-Ni4-O2	90.1(3)	O13-Ni7-O1	98.5(3)
O3-Ni2-O4	170.2(3)	O6-Ni4-O22	99.6(3)	N7-Ni7-O16	108.7(3)
N2-Ni2-O4	83.1(3)	N3-Ni4-O8	98.8(3)	O13-Ni7-O2	93.9(3)
O3-Ni2-O31	101.2(3)	O5-Ni4-O8	91.8(3)	N7-Ni7-O29	166.5(3)
N2-Ni2-O31	166.6(3)	O34-Ni4-O8	81.6(2)	O16-Ni7-O2	82.7(2)
O4-Ni2-O31	86.3(2)	O6-Ni4-O8	81.4(2)	O13-Ni7-O1	175.5(3)
O3-Ni2-O19	84.2(3)	O22-Ni4-O8	171.5(3)	N7-Ni7-O14	84.1(3)
N2-Ni2-O19	86.9(3)	N5-Ni5-O9	89.9(3)	O16-Ni7-O1	83.0(2)
O4-Ni2-O19	102.5(3)	N5-Ni5-O35	168.8(3)	O29-Ni7-O1	90.5(2)
O31-Ni2-O1	87.4(3)	O9-Ni5-O35	100.7(3)	O15-Ni8-N8	91.3(3)
O3-Ni2-O2	93.5(3)	N5-Ni5-O12	101.9(3)	O15-Ni8-O3	95.5(3)
N2-Ni2-O2	105.0(3)	O9-Ni5-O12	91.6(3)	N8-Ni8-O30	171.0(3)
O4-Ni2-O2	81.4(2)	O35-Ni5-O1	81.3(2)	O15-Ni8-O1	98.0(3)
O31-Ni2-O2	81.4(2)	N5-Ni5-O10	83.0(3)	N8-Ni8-O14	103.7(3)
O19-Ni2-O2	167.9(3)	O9-Ni5-O10	169.0(3)	O30-Ni8-O1	81.3(2)
N4-Ni3-O7	91.5(3)	O35-Ni5-O1	86.9(2)	O15-Ni8-O1	174.9(3)
N4-Ni3-O8	84.7(3)	O12-Ni5-O1	81.7(2)	N8-Ni8-O16	83.7(3)
O7-Ni3-O8	175.4(3)	N5-Ni5-O24	85.3(3)	O30-Ni8-O1	89.5(2)

Table S7. Major species assigned in the HRESI-MS of **1** and **2** in positive mode.

Complex **1** (In-Source CID 0 - 100 eV)		
Peaks	*Obs. m/z*	*Calc. m/z*
$[Dy_4Co_8(L)_6(OAc)_4(OH)_9(CH_3O)_2(H_2O)_3]^+$	2905.84	2905.80
$[Dy_4Co_8(L)_6(OAc)_4(OH)_9(CH_3O)_2(H_2O)_3(CH_3CH_2OH)]^+$	2951.78	2951.84
$[Dy_4Co_8(L)_6(OAc)_4(OH)_{10}(CH_3O)(H_2O)_2(CH_3CH_2OH)]^+$	2919.82	2919.87
$[Dy_4Co_8(L)_6(OAc)_4(OH)_{10}(CH_3O)(CH_3CH_2OH)_3(H_2O)]^+$	2994.87	2994.82
$[Dy_4Co_8(L)_6(OAc)_4(OH)_{11}(H_2O)_3]^+$	2876.74	2876.76
$[Dy_4Co_8(L)_6(OAc)_3(OH)_{11}(CH_3O)(H_2O)_2]^+$	2830.92	2830.85
$[Dy_4Co_8(L)_6(OAc)_2(OH)_{10}(CH_3O)_3]^+$	2782.76	2782.77
$[Dy_4Co_8(L)_6(OAc)_2(OH)_{11}(CH_3O)_2]^+$	2768.77	2707.72
$[Dy_4Co_8(L)_6(OAc)_2(OH)_{12}(CH_3O)]^+$	2753.74	2753.76
$[Dy_4Co_8(L)_6(OAc)_2(OH)_{11}(O)]^+$	2722.70	2722.78
$[Dy_4Co_8(L)_6(OAc)(O)_2(OH)_8(CH_3O)_2]^+$	2707.72	2707.77
$[Dy_4Co_8(L)_6(OAc)(O)_2(OH)_9(CH_3O)]^+$	2678.74	2678.71
$[Dy_4Co_8(L)_5(OAc)_4(OH)_7(O)_3(H_2O)_3]^+$	2644.74	2644.81
$[Dy_4Co_8(L)_5(OAc)_4(OH)_7(O)_3(CH_3CN)]^+$	2632.78	2632.54
$[Dy_4Co_8(L)_5(OAc)(HO)_9(O)_3(CH_3O)(H_2O)]^+$	2495.80	2495.73
$[Dy_4Co_8(L)_5(OAc)(OH)_{10}(O)_3(H_2O)]^+$	2481.75	2481.80
$[Dy_4Co_8(L)_5(O)_3(OH)_9(CH_3O)_2]^+$	2449.80	2449.84
Complex **2** (In-Source CID 0 eV)		
$[Dy_4Ni_8(L)_6(OH)_6(OAc)_2(O)_3(CH_3O)]^+$	2691.69	2691.66
$[Dy_4Ni_8(L)_5(OH)_5(OAc)_4(O)_3(CH_3O)_2(CH_3CN)]^+$	2655.70	2655.67
$[Dy_4Ni_8(L)_5(OH)_5(OAc)_4(O)_4(H_2O)_4]^+$	2640.71	2640.65
$[Dy_4Ni_8(L)_5(OAc)_4(OH)_4(O)_4(CH_3O)_2]^+$	2582.72	2582.76
$[Dy_4Ni_8(L)_5(OAc)_2(O)_3(OH)_8(CH_3O)(H_2O)]^+$	2551.62	2551.63
$[Dy_4Ni_8(L)_5(OAc)(O)_3(OH)_9(CH_3O)]^+$	2474.67	2474.64
$[Dy_4Ni_8(L)_5(OAc)(O)_3(OH)_{10}]^+$	2459.71	2459.76
$[Dy_4Ni_8(L)_4(OAc)_4(O)_4(OH)_6(CH_3O)(CH_3CN)]^+$	2444.63	2444.58

$[Dy_4Ni_8(L)_4 (O)_4(OH)_9(CH_3O)_2]^+$	2251.55	2251.58
$[Dy_4Ni_8(L)_4(OAc)(O)_4(OH)_9(H_2O)_2(CH_3CN)]^+$	2382.59	2382.60
$[Dy_4Ni_8(L)_4(OAc)(O)_4(OH)_7(CH_3O)_3(H_2O)]^+$	2325.69	2325.66
$[Dy_4Ni_8(L)_4(O)_4(OH)_6(CH_3O)]^+$	2236.49	2236.47

Table S8. Major species assigned in the Time-dependent HRESI-MS of **1** and **2** in positive mode.

Complex **1** (In-Source CID 0 eV)		
Peaks	*Obs. m/z*	*Calc. m/z*
$[Dy(HL)(HO)(H_2O)_4]^+$	466.02	466.05
$[Dy(HL)(HO)(H_2O)_2]^+$	431.00	431.04
$[DyCo(L)(OAc)_2(H_2O)_4(CH_3OH)(CH_3CN)]^+$	630.95	631.05
$[Dy_2Co(L)(OH)(O)(NO_3)(CH_3O)(H_2O)_4]^+$	797.01	797.04
$[Dy_3Co(L)(O)_2(NO_3)(CH_3O)(OH)_2]^+$	920.04	919.99
$[Dy_4CoL_2(OH)_2(O)_2(OAc)_2(NO_3)(CH_3CN)_2]^+$	1464.06	1464.09
$[Dy_4CoL_2(OH)_2(O)_2(OAc)_2(NO_3)(CH_3OH)(H_2O)]^+$	1429.85	1429.85
$[Dy_4Co_2L_3(OAc)_2(HO)_4(O)(CH_3O)]^+$	1640.88	1640.87
$[Dy_4Co_2L_3(O)_2(OAc)_3(HO)_2(H_2O)_3]^+$	1687.97	1687.88
$[Dy_4Co_4L_4(OH)_5(O)_3(CH_3CN)]^+$	1910.80	1910.85
$[Dy_4Co_8(L)_8(OAc)(OH)_{10}(CH_3OH)]^+$	3087.77	3087.83
$[Dy_4Co_8(L)_8(OAc)_2(OH)_9(CH_3OH)(H_2O)(CH_3CN)]^+$	3189.88	3189.86
Complex **2** (In-Source CID 0 eV)		
$[Ni(HL)]^+$	272.02	272.02
$[Dy_2NiL(OH)(O)(CH_3O)_2(CH_3OH)_2(CH_3CN)(H_2O)]^+$	816.02	816.00
$[Dy_3Ni(L)_2(O)_3(CH_3OH)(H_2O)_2]^+$	1088.05	1088.04
$[Dy_3NiL_2(O)_3(CH_3OH)(H_2O)_2]^+$	1359.07	1359.00
$[Dy_4Ni_2(L)_3(OH)_3(O)_3(H_2O)_2]^+$	1538.08	1538.07
$[Dy_4Ni_2(L)_3(OH)_3(O)_3(CH_3OH)(CH_3CN)(H_2O)_3]^+$	1630.86	1630.87
$[Dy_4Ni_4(L)_3(OH)_3(O)_5(CH_3OH)(H_2O)]^+$	1503.82	1503.80
$[Dy_4Ni_4(L)_3(OH)_3(O)_5(CH_3OH)_2(H_2O)]^+$	1735.08	1735.07
$[Dy_4Ni_6(L)_4(OH)_6(O)_4(CH_3O)(H_2O)_3(CH_3OH)]^+$	1916.61	1917.60

$[Dy_4Ni(L)_2(OH)_3(O)_3(CH_3OH)_5(CH_3CN)(H_2O)]^+$	1452.97	1452.91
$[Dy_4Ni(L)_2(OH)_3(O)_3(CH_3OH)(CH_3CN)_2(H_2O)]^+$	1462.99	1462.97
$[Dy_4Ni_8(L)_8(OAc)_3(OH)_8(CH_3OH)(H_2O)_4]^+$	3238.91	3238.89
$[Dy_4Ni_8(L)_8(OAc)_3(OH)_8(CH_3CN)_3]^+$	3258.85	3258.79

Table S9. Major species assigned in the HRESI-MS of **1** and **2** in positive mode

Fragments	Relative Intensity						
	5min	40min	2h	6h	10h	14h	16h
$[DyL(solv.)]^+$	0.90	0.50	0.81	0.30	0.11	0.10	0.00
$[DyCoL(solv.)]^+$	0.40	0.73	0.80	0.21	0.13	0.21	0.00
$[Dy_2CoL(solv.)]^+$	0.01	0.10	0.90	0.80	0.62	0.20	0.010
$[Dy_3CoL]^+$	0.30	0.40	0.60	0.70	0.71	0.64	0.03
$[Dy_4CoL_2(solv.)]^+$	0.08	0.40	0.71	0.41	0.70	0.61	0.08
$[Dy_4Co_2L_3(solv.)]^+$	0.10	0.40	0.61	0.35	0.74	0.41	0.32
$[Dy_4Co_4L_4(solv.)]^+$	0	010	0.51	0.81	0.83	0.65	0.50
$[Dy_4Co_8L_8(solv.)]^+$	0	0.21	0.40	0.40	0.91	0.80	0.90
$[NiL(solv.)]^+$	0.80	0.82	0.91	0.60	0.51	0.41	0.30
$[Dy_2NiL_2(solv.)]^+$	0.30	0.31	0.82	0.21	0.12	0.21	0.41
$[Dy_3NiL_2(solv.)]^+$	0	0.11	0.90	0.80	0.61	0.21	0.20
$[Dy_4NiL_2(solv.)]^+$	0	0.40	0.60	0.70	0.70	0.41	0.03
$[Dy_4Ni_2L_3(solv.)]^+$	0	0.40	0.70	0.40	0.71	0.60	0.08
$[Dy_4Ni_4L_4(solv.)]^+$	0	0.41	0.90	0.30	0.70	0.41	0.31
$[Dy_4Ni_6L_4(solv.)]^+$	0	0.10	0.12	0.81	0.80	0.65	0.30
$[Dy_4Ni_8L_8(solv.)]^+$	0	0.20	0.10	0.1	0.20	0.32	0.90

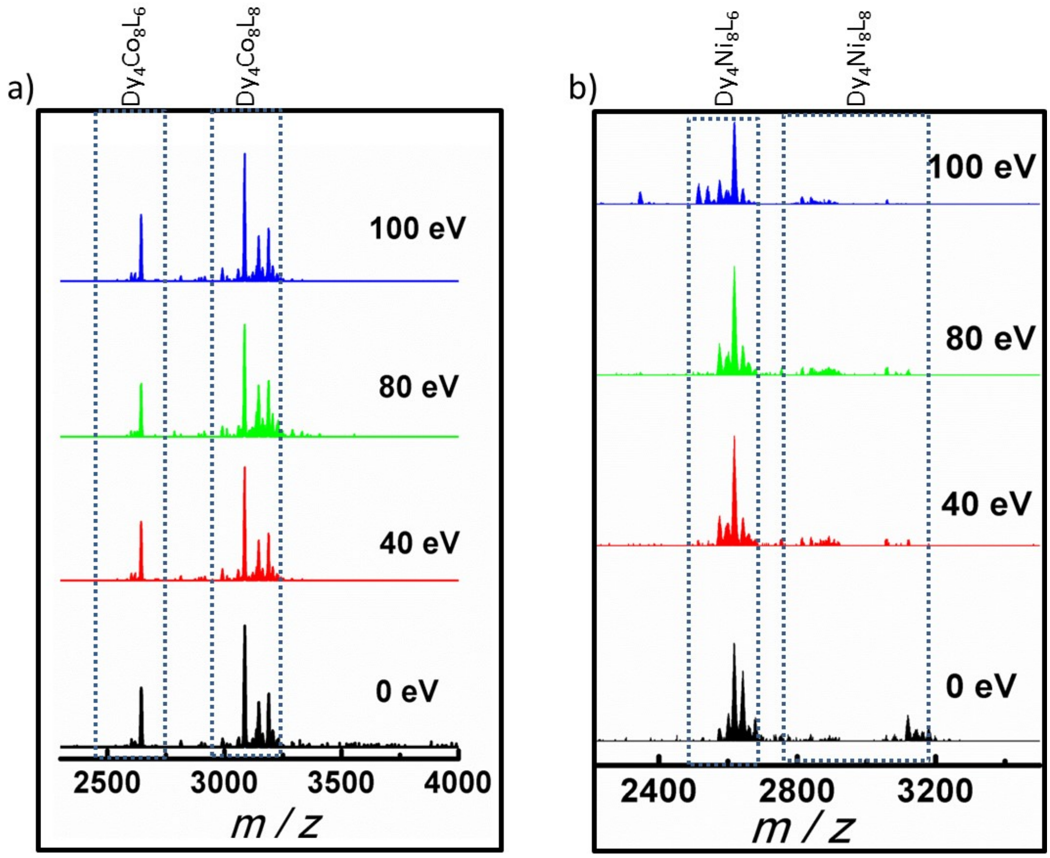

Fig. S12. Molecular ion peaks of 1 (a) and 2 (b) in cation modes obtained by HRESI-MS test with different ion source voltages (0, 40, 80 and 100 eV).

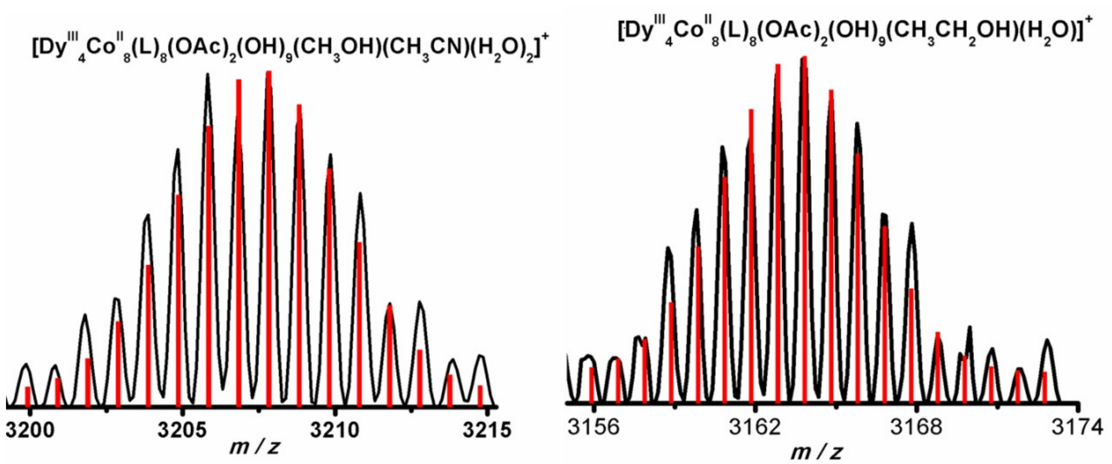

Fig. S13. The superposed simulated and observed spectra of several species for **1** (In-Source CID 0 -100 eV).

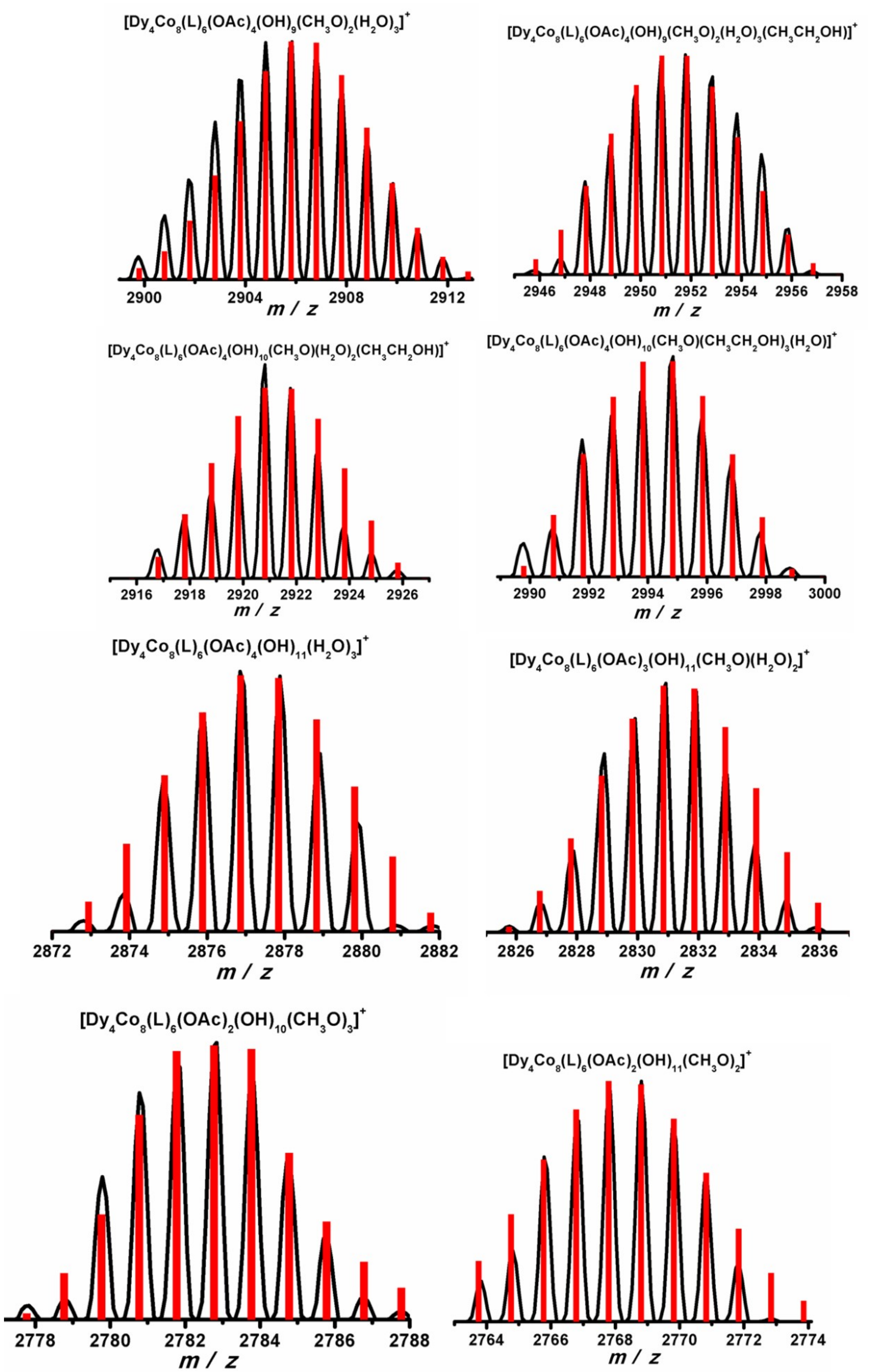

Fig. S14. The superposed simulated and observed spectra of several species for **1** (In-Source CID 0 -100 eV).

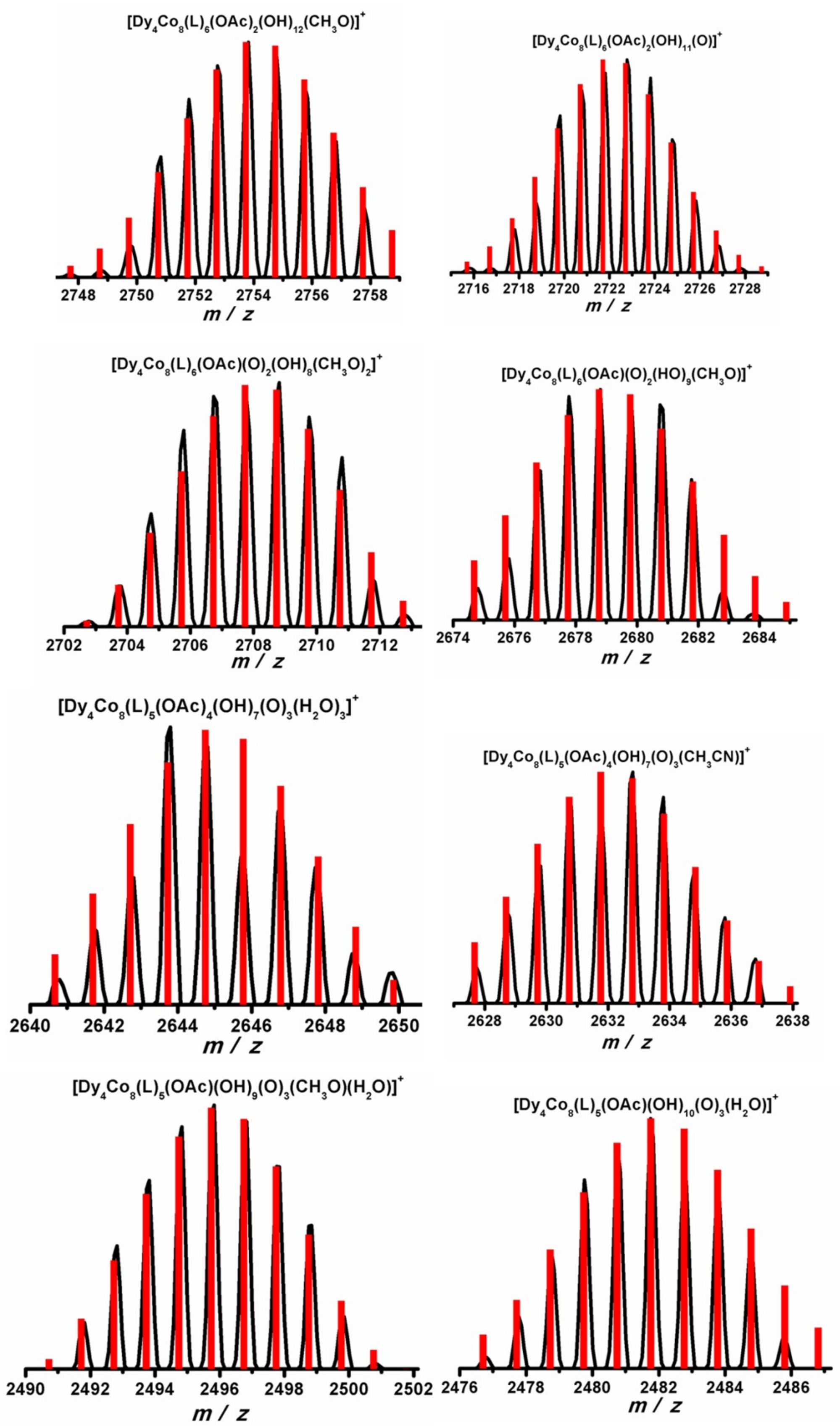

Fig. S15. The superposed simulated and observed spectra of several species for **1** (In-Source CID 0 -100 eV).

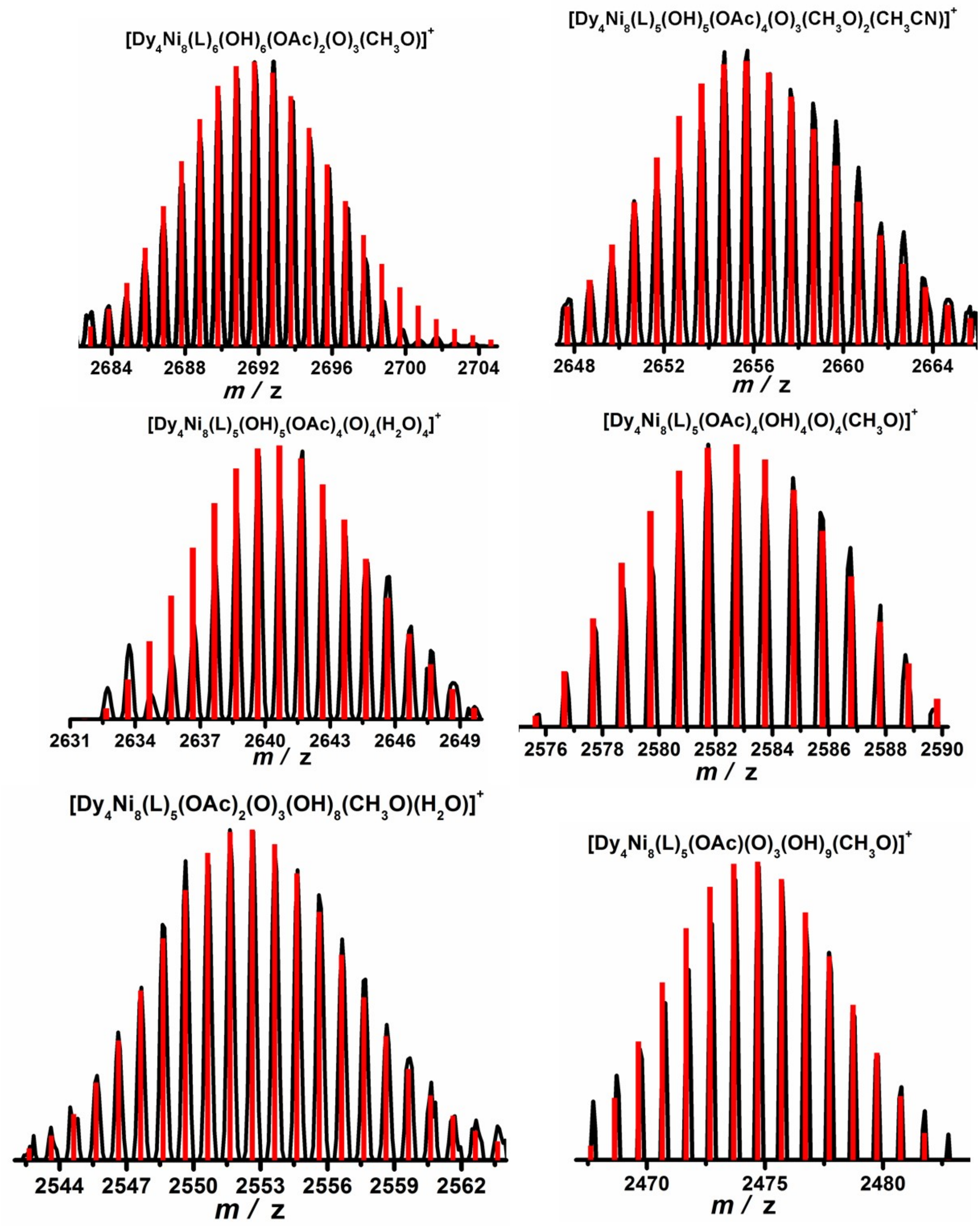

Fig. S16. The superposed simulated and observed spectra of several species for **2** (In-Source CID 0 -100 eV).

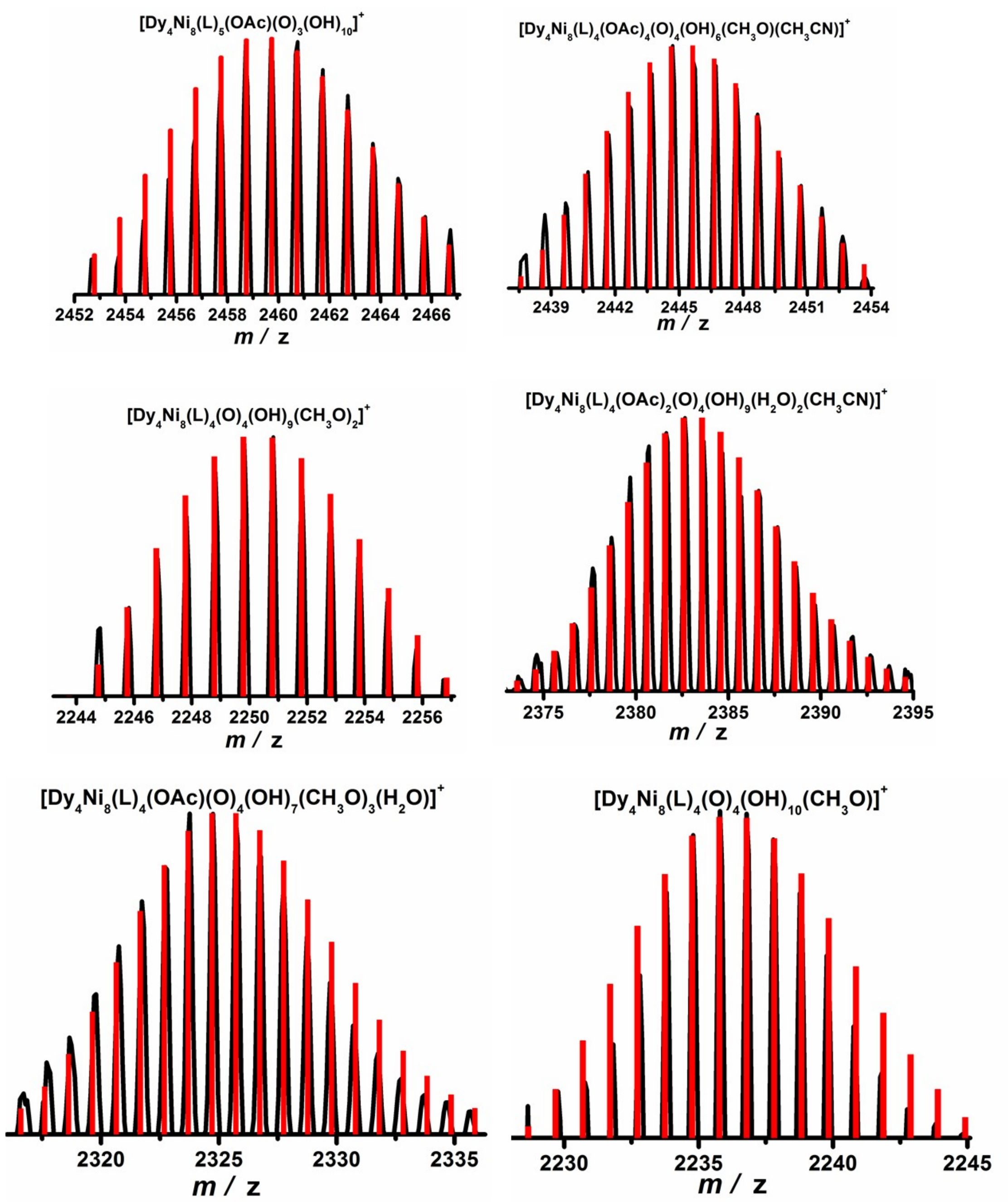

Fig. S17. The superposed simulated and observed spectra of several species for **2** (In-Source CID 0 -100 eV).

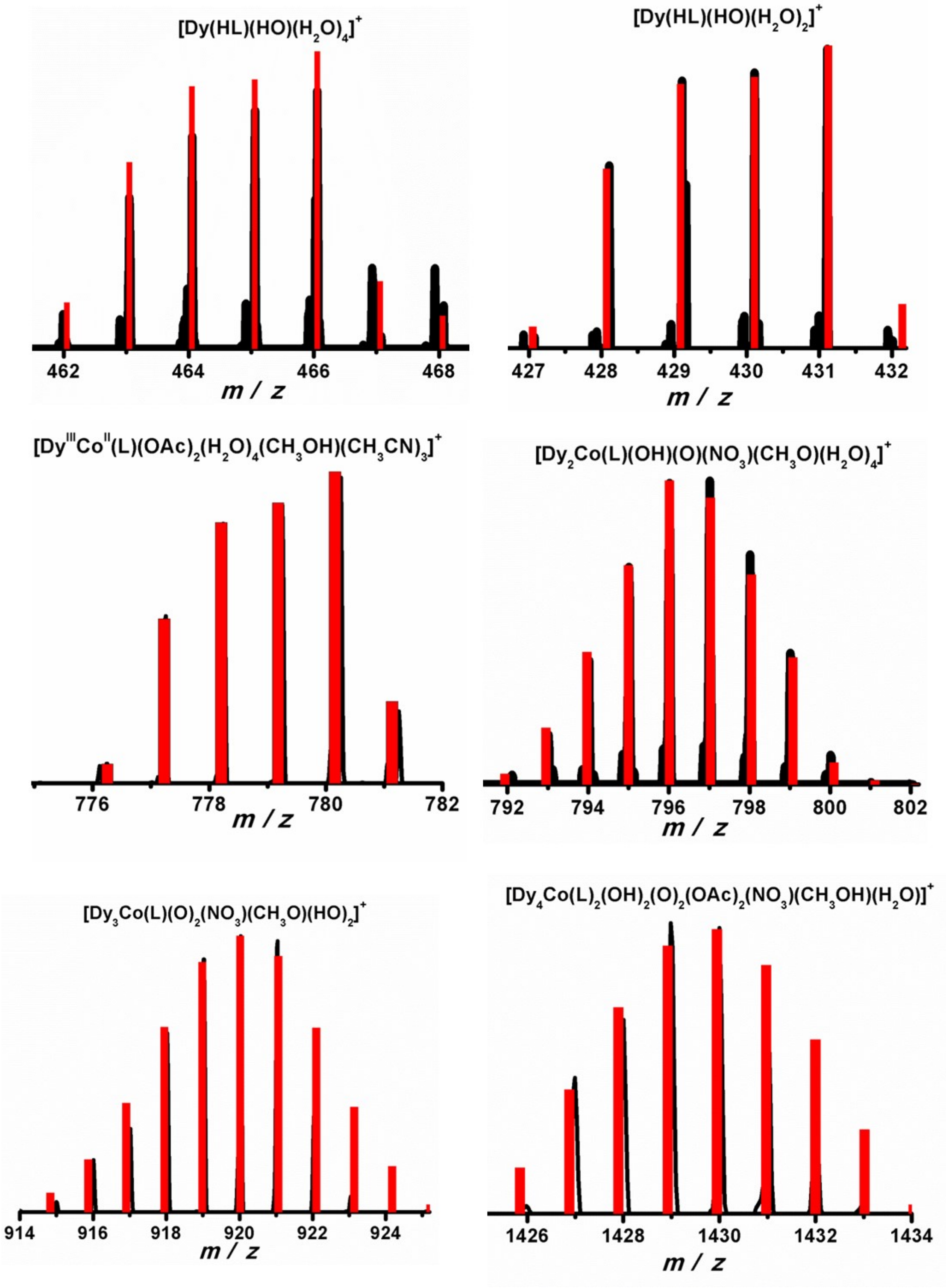

Fig. S18. The superposed simulated and observed spectra of several species in the Time-dependent ESI-MS of **1**.

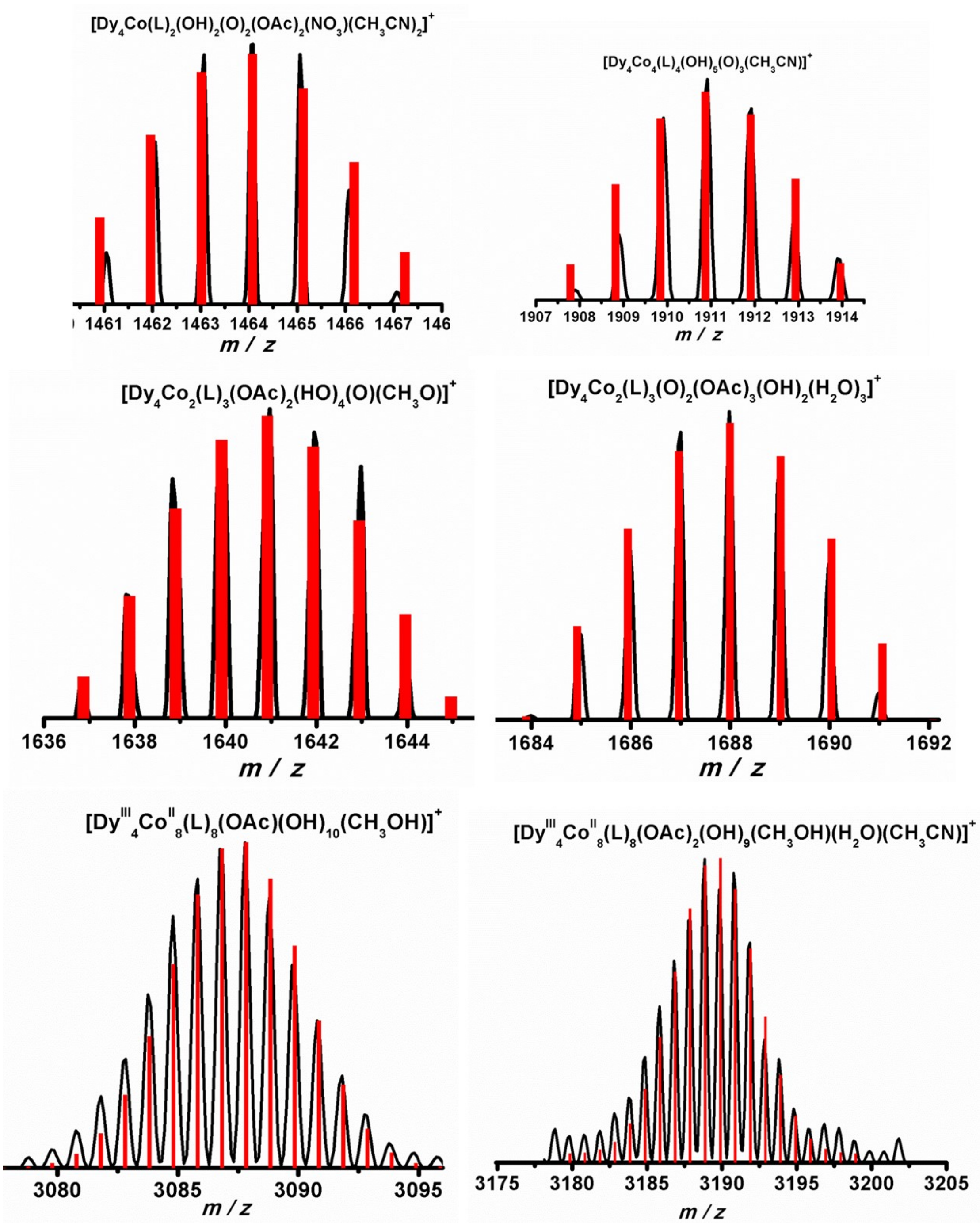

Fig. S19. The superposed simulated and observed spectra of several species in the Time-dependent ESI-MS of **1**.

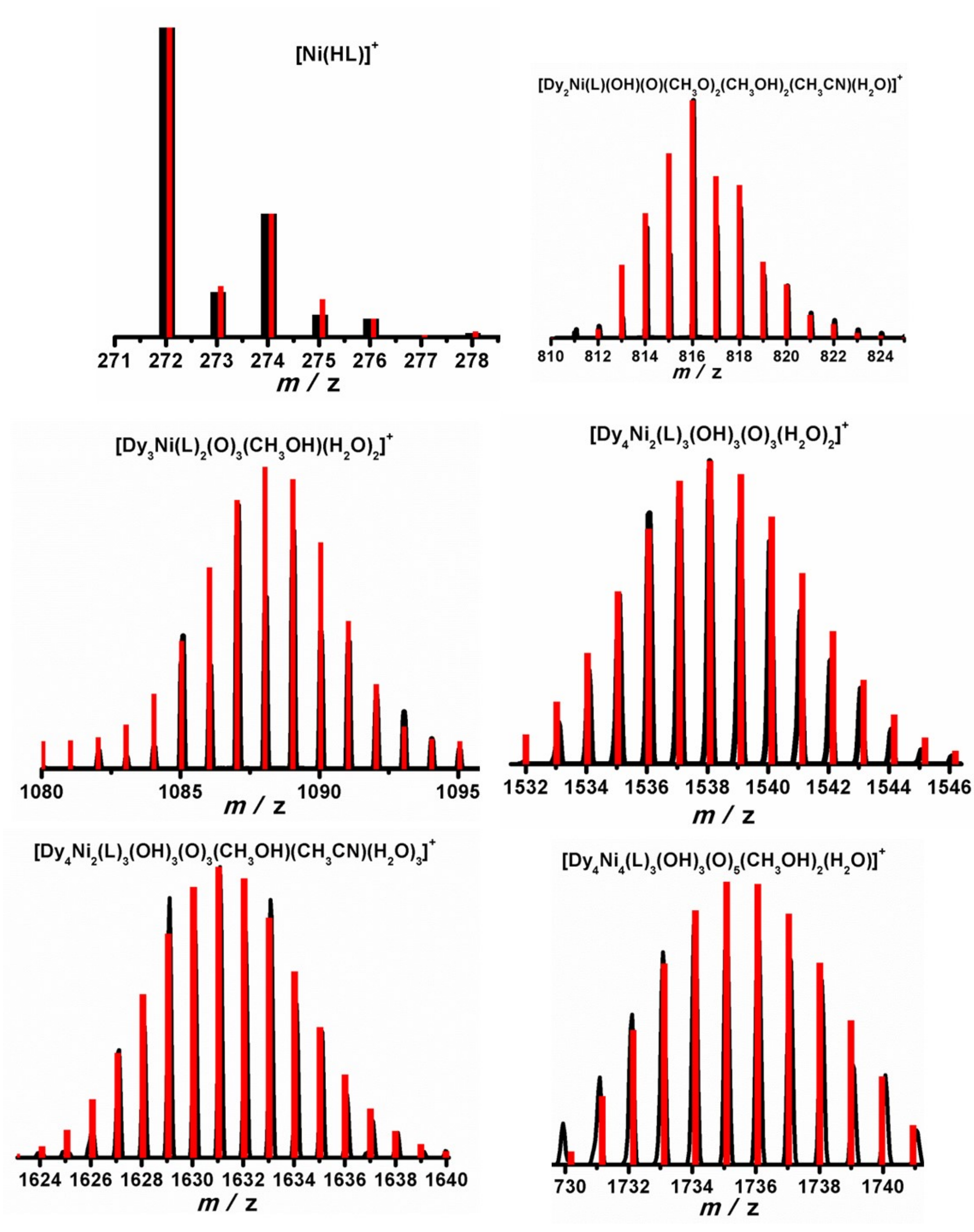

Fig. S20. The superposed simulated and observed spectra of several species in the Time-dependent ESI-MS of **2**.

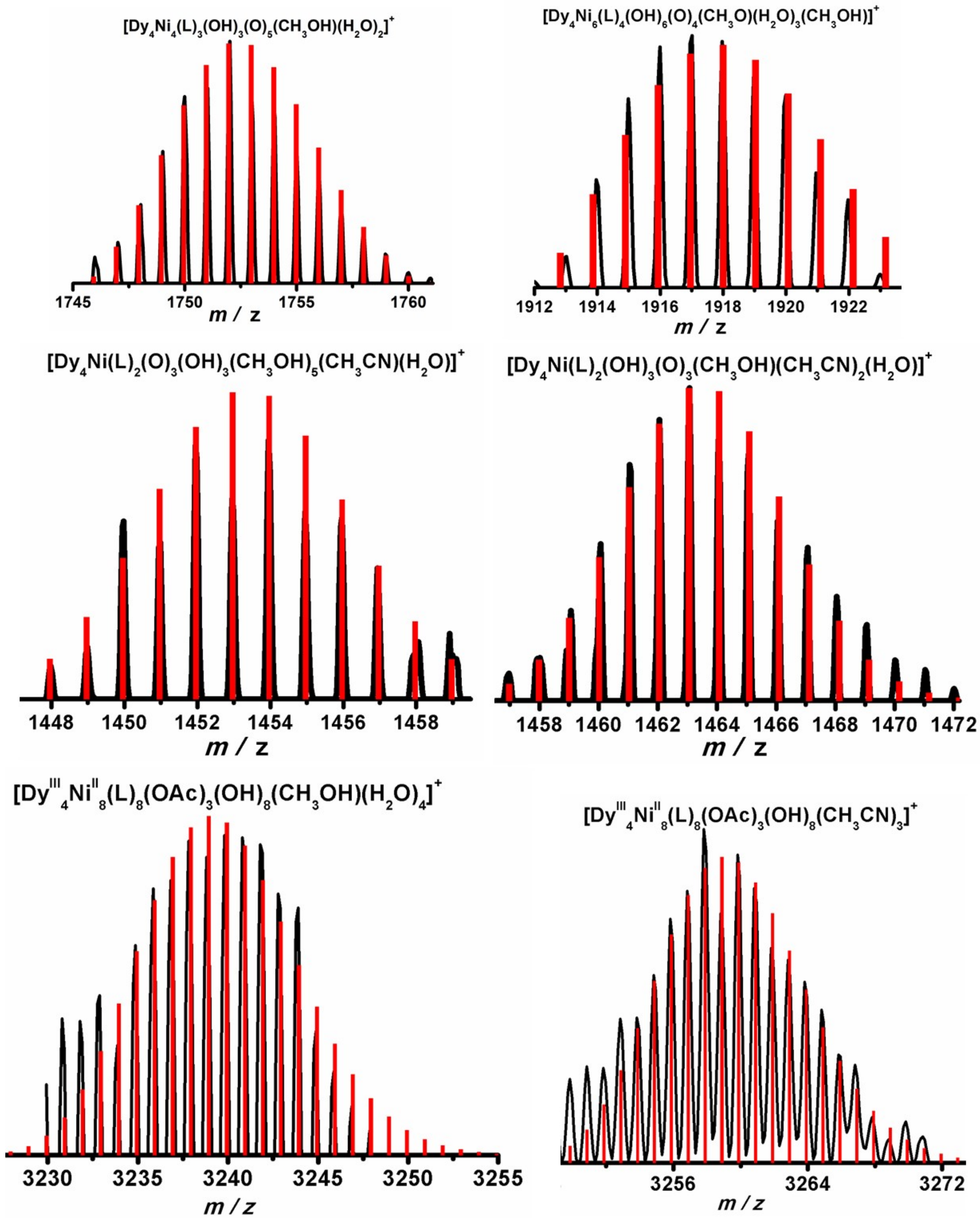

Fig. S21. The superposed simulated and observed spectra of several species in the Time-dependent ESI-MS of **1**.

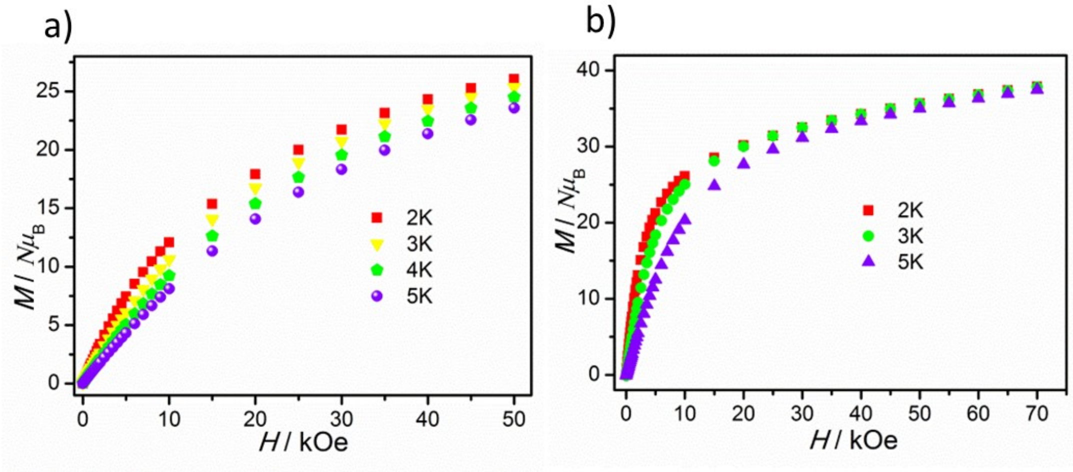

Fig. S22. Plots of *M vs*. *H* for complex **1** (a) and **2** (b) measured at 2-5 K.

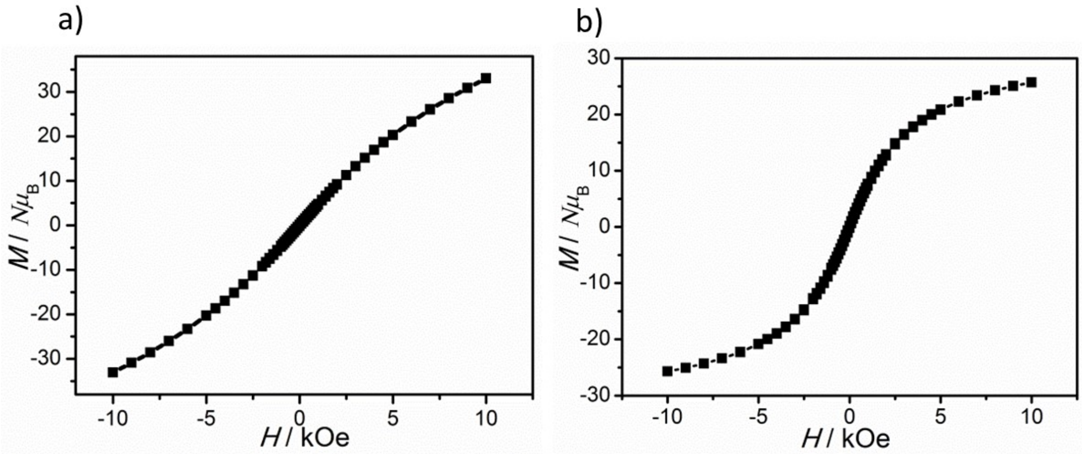

Fig. S23. Plots of Magnetic hysteresis loops for **1** (a) and **2** (b).

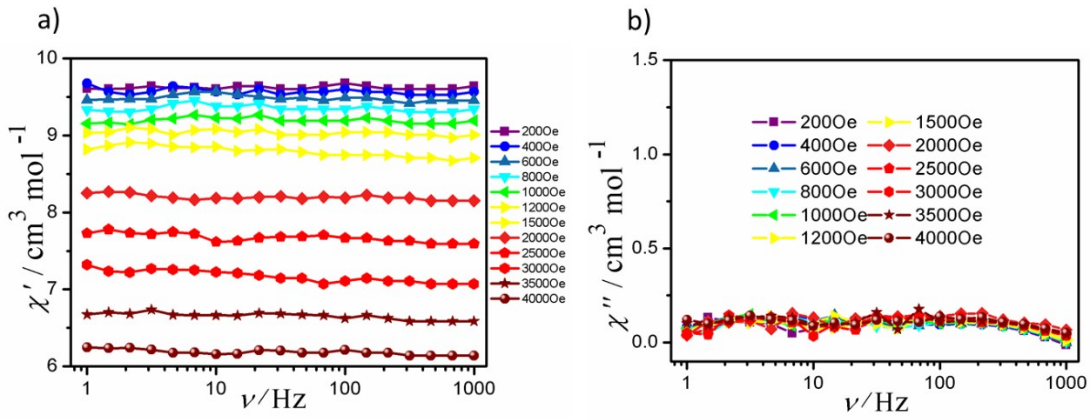

Fig. S24. Plots of χ’ and χ” vs v at 2-5.0 K under different dc field of 0 Oe for **1**.

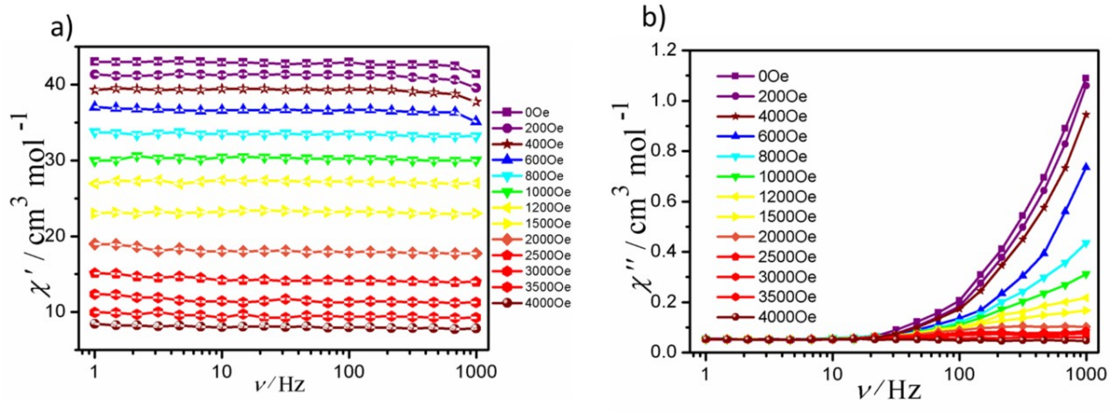

Fig. S25. Plots of χ' and χ'' vs v at 2-5.0 K under different dc field of 0 Oe for **2**.

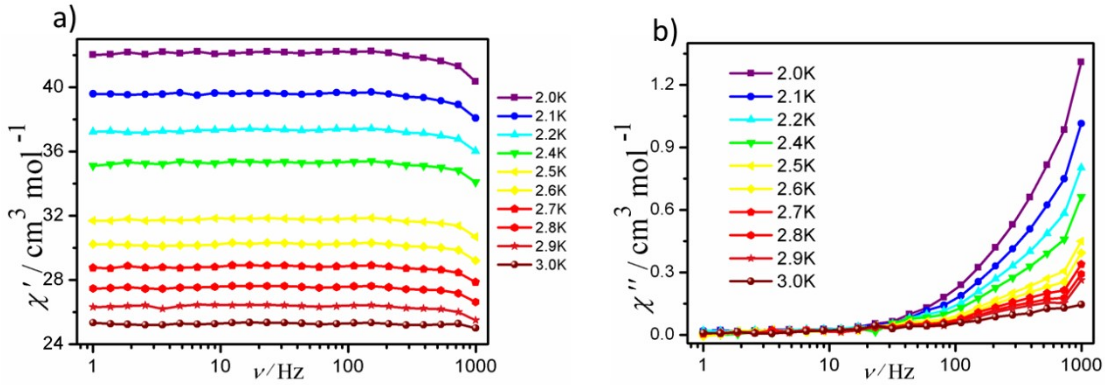

Fig. S26. Plots of χ' (a) and χ'' (a) vs v at 2-3.0 K under a dc field of 0 Oe for **2**.

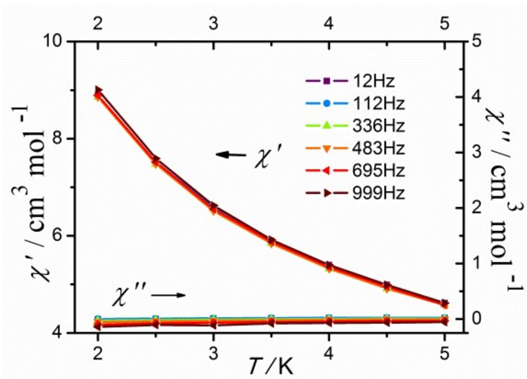

Fig. S27. Temperature-dependent χ' and χ'' ac susceptibilities under zero dc field for **1**.

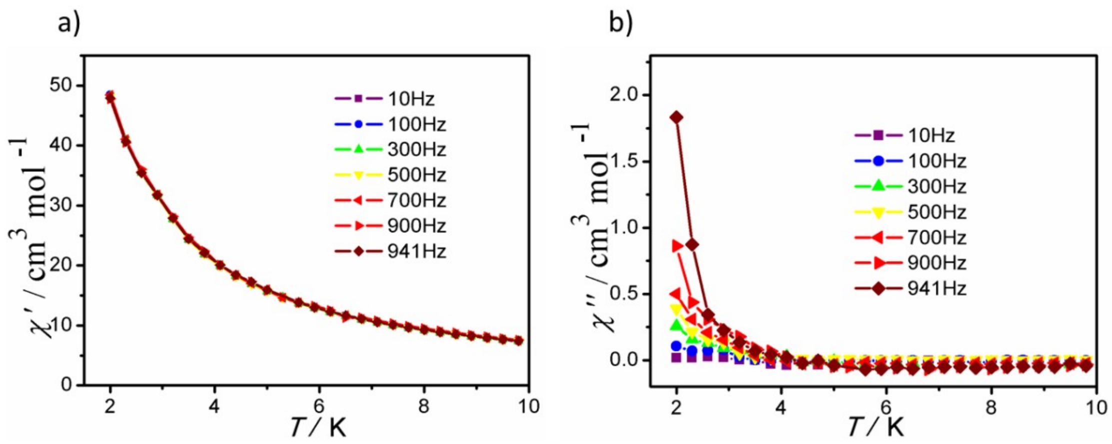

Fig. S28. Temperature-dependent χ' (a) and χ'' (b) ac susceptibilities under zero dc field for **2**.

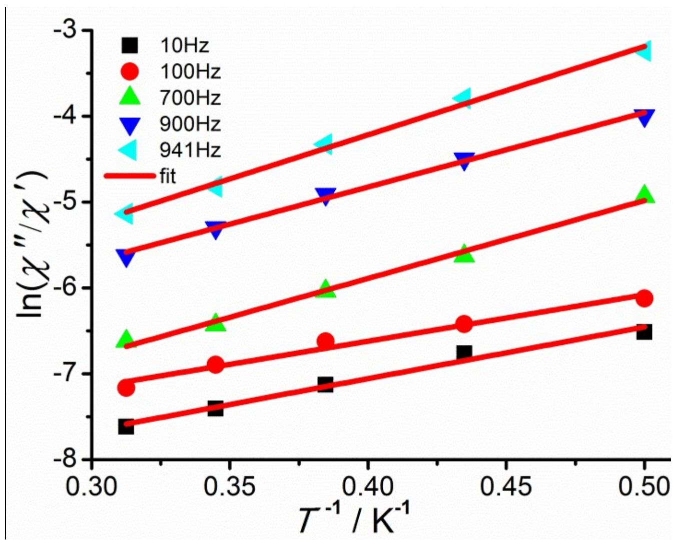

Fig. S29. Plots of ln(χ''/χ') vs. 1/T for 2 under 0 Oe dc field, the solid lines represent the best fits.